Local quenches in fracton field theory: Lieb-Robinson bound, noncausal dynamics and fractal excitation patterns

Dmitry S. Ageev[1,*], Andrey A. Bagrov[2,†], Aleksandr I. Belokon[1,‡], Askar Iliasov[2,§]
Vasilii V. Pushkarev[1,∥] and Femke Verheijen[2]

[1]*Steklov Mathematical Institute of Russian Academy of Sciences*, 8 Gubkina st., Moscow 119991, Russia
[2]*Institute for Molecules and Materials, Radboud University*, Heyendaalseweg 135,
6525AJ Nijmegen, The Netherlands

We study the out-of-equilibrium dynamics induced by a local perturbation in fracton field theory. For the $\mathbb{Z}_4$- and $\mathbb{Z}_8$-symmetric free fractonic theories, we compute the time dynamics of several observables such as the two-point Green's function, $\langle \phi^2 \rangle$ condensate, energy density, and the dipole momentum. The time-dependent considerations highlight that the free fractonic theory breaks causality and exhibits instantaneous signal propagation, even if an additional relativistic term is included to enforce a speed limit in the system. We show that it is related to the fact that the Lieb-Robinson bound does not hold in the continuum limit of the fracton field theory, and the effective bounded speed of light does not emerge. For the theory in finite volume, we show that the fracton wave front acquires fractal shape with nontrivial Hausdorff dimension and argue that this phenomenon cannot be explained by a simple self-interference effect.

I. INTRODUCTION

Fractons are conjectural states of matter possessing a number of exotic properties that do not allow us to describe them within the conventional framework of quantum many-body theory using such concepts as symmetry breaking, band structures, quasiparticles, or topological phases [1–6]. Continuum fractonic models—fracton quantum field theories—have been analyzed in detail [7–10] and were shown to be very distinct in many regards from their relativistic counterparts.

Foremost, since the lattice theory spectrum consists of immobile particles or particles with restricted mobility, which are called fractons, at the level of the low-energy theory, there are local defects, whose locations are restricted.

Also, the ground-state degeneracy of the system on a lattice scales exponentially with the system size and hence diverges in the continuum limit. Therefore, the continuum version of the theory possesses an infinite number of ground states. In particular, this leads to UV/IR mixing, which means that a low-energy observer is sensitive to short-distance physics. This is a challenge because a continuum field theory is usually expected to give a consistent description of low-energy physics, which does not depend on its UV completion.

Finally, even though fracton field theories are neither Lorentz invariant nor $SO(2)$ rotationally invariant, they possess exotic global symmetries, including subsystem symmetries such that their charges act differently in different subspaces of the total space.

Given the very peculiar property of restricted mobility, out-of-equilibrium dynamics of such systems can be highly nontrivial and not resembling that of regular isotropic or smoothly anisotropic theories. By quenching a fracton field theory, one can get deeper insight into its response properties and unveil features that cannot be deduced from equilibrium considerations.

In quantum field theory (QFT), quenches have been extensively studied in a number of diverse settings. The number of exactly solvable models is restricted and mainly includes conformal field theories (CFTs) [11–15]. Some other results were obtained for free field theories and the simplest interacting theories [16–25]. At the same time, the study of global quench setups is promising as demonstrated by their intensive exploration in terms of AdS/CFT correspondence as a model of thermalization [26–30].

In Ref. [25], some of the authors of this paper initiated analysis of time-dependent properties of fractonic matter by considering a global quench in fracton field theory, where

[*]Contact author: ageev@mi-ras.ru
[†]Contact author: andrey.bagrov@ru.nl
[‡]Contact author: belokon@mi-ras.ru
[§]Contact author: askar.iliasov@ru.nl
[∥]Contact author: pushkarev@mi-ras.ru

the behavior of the two-point correlation function after the abrupt change of system parameters as well as after an abrupt change of the symmetry of the theory has been analyzed. However, global perturbation of the theory reveals its homogeneous temporal dynamics, but not the spatiotemporal properties, which become visible in the scenario of inhomogeneous—local—quench. Hence, in the present paper, we continue this research line and study the dynamics of the fracton field subject to a local perturbation. Our goal is to see how the structure of fractonic theories affects the propagation of local excitations. To contextualize our findings, we put the observables calculated for the fracton field theory in comparison with those in locally quenched relativistic field theory.

In a local quench prescription, the initial state of the system is perturbed locally at one (single quench) or several points (double quench, triple quench, etc.), and its subsequent evolution is reflected in the behavior of quantum mechanical observables—correlation functions. Local quenches have recently been studied in various theoretical areas, such as condensed matter theory [31–36], entanglement and quantum gravity [37–41], and complexity and chaos [42].

The so-called geometric quench introduced in Ref. [12] involves joining two different theories with a boundary at some time moment. In Ref. [43], an attempt is made to generalize this setup to a higher-dimensional case. Another example is the operator local quench, which is a setup describing creating a localized excited state prepared by inserting a local operator into the path integral that defines the state [40]. Even though localized excited states have been studied in diverse contexts [38–40,42,44–68], most of the known examples of local quenches are related to two-dimensional CFT [45,46,63,69]. Recently, we have studied operator local quenches in massive scalar field theory [70], which is a natural extension of earlier considerations [38], where the form of observables after a local excitation was completely fixed by conformal symmetry. The method of the straightforward calculation of correlators using Wick's theorem, proposed in this work, allows us to rederive previously known results and study QFTs with arbitrary interactions without having to confine ourselves to considering only conformal theories. Also, conformal derivation was limited to two dimensions, while this approach works in arbitrary dimensions. The latter fact, in particular, makes it possible to rederive the results obtained earlier in holographic correspondence AdS_{d+1}/CFT_d, where the time evolution of the state on the CFT_d side is dual to a falling massive particle in AdS_{d+1} ($d + 1$-dimensional anti-de Sitter spacetime) [69].

In this paper, we rely on this approach to study operator local quenches in $2 + 1$-dimensional fracton field theory, which is a low-energy limit [8] of the XY-plaquette model [71]. In the latter theory, a compact scalar field, $\phi_s \sim \phi_s + 2\pi$, is defined on each site s of a periodic square

lattice with spacing a and the number of sites L^x and L^y in the x and y direction, correspondingly. Its Hamiltonian reads [8]

$$H = \frac{u}{2} \sum_s \pi_s^2 - K \sum_s \cos{(\Delta_{xy} \phi_s)}, \qquad (1)$$

where π_s denotes conjugate momenta of the scalar field, and

$$\Delta_{xy} \phi_{\hat{x}, \hat{y}} = \phi_{\hat{x}+1, \hat{y}+1} - \phi_{\hat{x}+1, \hat{y}} - \phi_{\hat{x}, \hat{y}+1} + \phi_{\hat{x}, \hat{y}}.$$

The coordinates $(\hat{x}, \hat{y})$ are integer labels of the sites, $\hat{x} = 1, ..., L^x$ and $\hat{y} = 1, ..., L^y$. Hamiltonian (1) is invariant under momentum dipole symmetries [which are $U(1)_i$ subsystem symmetries along ith coordinate line on the lattice, $\phi_s \to \phi_s + \varphi$] as well as under $\mathbb{Z}_4$ rotations of the lattice. The continuum limit of the XY-plaquette model is achieved by taking the double limit $a \to 0, L^i \to \infty$ such that product aL^i is kept fixed. The resulting Lagrangian density is given by [8]

$$\mathcal{L} = \frac{\mu_0}{2} (\partial_t \phi)^2 - \frac{1}{2\mu} (\partial_x \partial_y \phi)^2, \quad [\phi] = 0, \quad [\mu_0], [\mu] = 1, \quad (2)$$

where μ_0 and μ are parameters with mass dimension $+1$. The $U(1)_i$ symmetries of the lattice model become in the continuum limit a momentum dipole symmetry $\phi(t, x, y) \to \phi(t, x, y) + f_x(x) + f_y(y)$ for arbitrary functions f_x and f_y. The symmetry under $\mathbb{Z}_4$ spatial rotations is preserved in the continuum limit.

The paper is organized as follows. In Sec. II, we review the operator local quench protocol and the fracton field theory we are studying. The postquench dynamics of the two-point function is described in Sec. III, and the dynamics of the energy and dipole momentum densities is described in Sec. IV. In Sec. V, we show that the Lieb-Robinson bound of a discretized fractonic theory does not support the emergence of the finite speed of light in the continuous theory. In Sec. VI, we generalize our considerations onto the finite volume case. In Sec. VII, we comment on the fractal structure of the excitations in the locally quenched theory in finite volume. We also note there that there is a considerable difference between local and global quench setups in fractal behavior of the corresponding excitations. Section VIII is an outlook.

II. SETUP

A. Operator local quench

An insertion of a local operator O at spacetime point (t_0, x_0) creates an excited state $|\Psi(t)\rangle$ evolving in time,

$$|\Psi(t)\rangle = \mathcal{N}_O \cdot e^{-iH(t-t_0)} \cdot e^{-\varepsilon H} O(t_0, x_0)|0\rangle, \qquad (3)$$

where $\mathcal{N}_O$ is a normalization factor, which ensures that $\langle\Psi|\Psi\rangle = 1$, and the UV regularization parameter ε preserves a finite norm of the state. Choosing $(t_0, x_0) = (0,0)$, the evolution of some observable $\mathcal{O}$ after the single-point local quench (3) reduces to a three-point Lorentzian correlation function:

$$\langle\mathcal{O}(t,x)\rangle_O = \frac{\langle 0|O^\dagger(i\varepsilon,0)\mathcal{O}(t,x)O(-i\varepsilon,0)|0\rangle}{\langle 0|O^\dagger(i\varepsilon,0)O(-i\varepsilon,0)|0\rangle}. \quad (4)$$

To evaluate it, it is easier to perform calculations in imaginary time and then transform the result to real times by Wick rotation $t \to -i\tau$.[1] Usually, the observable $\mathcal{O}$ is a composite operator, and the calculation requires regularization. One of the possibilities is the point-splitting scheme, where the spacetime point, at which the observable is defined, is split into two separated ones, and then the correlation function (4) is calculated using Wick's contractions [70]. The final correlation function consists of a finite part and a term, which in the limit of merging points contains a constant and a divergence. The sum of the finite part and the constant is interpreted as the actual value of the observable, while the divergent part is discarded (i.e., the correlator is renormalized). For example, in the case of the two-dimensional CFT stress-energy tensor, the constant coming from the point splitting corresponds to the anomalous term in its transformation law [70].

At this point, we do not consider theories with interactions, but only free field theories, in which all information is encoded in the two-point correlation functions. In momentum space, it means that the theory is completely determined by its dispersion relation. We will use this machinery to study local quenches in a free QFT with discrete rotational symmetries—the massive scalar fracton field theory.

B. Fracton field theory

In this paper, we consider scalar fracton field theories introduced in Ref. [25] with underlying $\mathbb{Z}_n$ symmetry and a relativistic and a mass terms added for the purpose of regularization. This $\mathbb{Z}_n$ invariance translates into the following Euclidean dispersion relation[2]:

$$\omega^2 = -\frac{1}{\mu_0}\left[\epsilon(k^2 + q^2) + \frac{f_\alpha(k,q)}{\mu} + \mu m^2\right], \qquad [\epsilon] = 1,$$

$$[f_\alpha] = 4, \qquad \alpha = \frac{n}{4}. \quad (5)$$

The function $f_\alpha(k, q)$ of momenta k and q reflects the underlying symmetry of the theory. We also assume that this general form of the dispersion relation includes a rotationally invariant part $\epsilon(k^2 + q^2)$ which tames the divergences corresponding to the UV/IR mixing of fractonic theories, i.e., when $k \to \infty$ and $q \to 0$ or vice versa, and a mass term, which regulates IR divergences, when both k and q tends to 0.

In coordinate space, function f_α corresponds to higher-derivative operators in the action. In the case of $n = 2$, the expression for f_α is given by $k^2 q^2$ as follows from Ref. [8]. For higher orders, the expression for $f_\alpha(k, q)$ can be derived through the transformation to polar coordinates with stretched angular coordinate, $k = \sqrt{k^2 + q^2}\cos(\alpha\varphi)$ and $q = \sqrt{k^2 + q^2}\sin(\alpha\varphi)$. The result is given by [25]

$$f_\alpha = (k^2 + q^2)^2\cos^2(\alpha\varphi)\sin^2(\alpha\varphi)$$

$$= \left[\frac{(k + iq)^{4\alpha} - (k^2 + q^2)^{2\alpha}}{4(k^2 + q^2)^{\alpha-1}(k + iq)^{2\alpha}}\right]^2. \quad (6)$$

Specific examples of such fracton free field theories include:

(i) $\mathbb{Z}_4$-symmetric theory, which is invariant under 90° spatial rotations. The Euclidean action is given by the low-energy limit of the XY-plaquette lattice model (2) with an added relativistic and a mass term

$$S = \frac{A}{2}\int d\tau dx dy\left(\mu_0(\partial_\tau\phi)^2 + \epsilon(\partial_x\phi)^2\right.$$

$$\left. + \epsilon(\partial_y\phi)^2 + \frac{1}{\mu}(\partial_x\partial_y\phi)^2 + \mu m^2\phi^2\right), \quad (7)$$

where A is a normalization constant that we keep here for generality but fix it to be equal to $1/(4\pi)$ in the calculations. The global momentum dipole symmetry of the original theory is now broken by the presence of mass. The dispersion relation is given by (5) with $\alpha = 1$ (see Appendix A for details)

$$\omega^2 = -\frac{1}{\mu_0}\left[\epsilon(k^2 + q^2) + \frac{k^2 q^2}{\mu} + \mu m^2\right]. \quad (8)$$

(ii) $\mathbb{Z}_8$-symmetric theory, which is invariant under 45° rotations. The dispersion relation is given by (5) with $\alpha = 2$,

$$\omega^2 = -\frac{1}{\mu_0}\left[\epsilon(k^2 + q^2) + \frac{4(k^3 q - k q^3)^2}{\mu(k^2 + q^2)^2} + \mu m^2\right]. \quad (9)$$

III. DYNAMICS OF TWO-POINT FUNCTION AND ϕ^2 CONDENSATE

In free theory, the dynamics is fully determined by the behavior of two-point correlation functions. Hence, two cases with different properties can be studied: i. when two

---

[1] For a discussion on analytical continuation, we refer the reader to Appendix A of Ref. [70].

[2] Note that in the $d = 3$ case the field ϕ has zero mass dimension (2). This means that the coefficient before the ϕ^2 term has mass dimension $3/2$. We write this coefficient as μm^2 to deal with the usual dimension-1 mass parameter m, using μ to add up one more dimension, so that $[\mu m^2] = 3$.

operators are defined at different spacetime points and ii. when they are defined at the same point—the so-called ϕ^2 condensate. In this paper, we will consider local quenches corresponding to the insertion of ϕ operator.

Let us define equal-time two-point correlation function with the equilibrium part subtracted, namely,

$$G(t, x, y) \equiv \frac{\langle 0|\phi(i\varepsilon, 0, 0)\phi(t, x, y)\phi(t, 0, 0)\phi(-i\varepsilon, 0, 0)|0\rangle}{\langle 0|\phi(i\varepsilon, 0, 0)\phi(-i\varepsilon, 0, 0)|0\rangle} - \langle \phi(t, x, y)\phi(t, 0, 0)\rangle. \tag{10}$$

A similar one was studied before in the context of global quenches [17,18,25] and represents a perturbation of the two-point function caused by quench excitation. By the Wick theorem, it transforms to

$$G(t, x, y) = \frac{\langle 0|\phi(i\varepsilon, 0, 0)\phi(t, x, y)|0\rangle\langle 0|\phi(t, 0, 0)\phi(-i\varepsilon, 0, 0)|0\rangle}{\langle 0|\phi(i\varepsilon, 0, 0)\phi(-i\varepsilon, 0, 0)|0\rangle}$$

$$+ \frac{\langle 0|\phi(i\varepsilon, 0, 0)\phi(t, 0, 0)|0\rangle\langle 0|\phi(t, x, y)\phi(-i\varepsilon, 0, 0)|0\rangle}{\langle 0|\phi(i\varepsilon, 0, 0)\phi(-i\varepsilon, 0, 0)|0\rangle}. \tag{11}$$

Calculating Wick's contractions using the two-point function in mixed representation (A6), we get

$$\langle 0|\phi(i\varepsilon, 0, 0)\phi(t, x, y)|0\rangle\langle 0|\phi(t, 0, 0)\phi(-i\varepsilon, 0, 0)|0\rangle + \langle 0|\phi(i\varepsilon, 0, 0)\phi(t, 0, 0)|0\rangle\langle 0|\phi(t, x, y)\phi(-i\varepsilon, 0, 0)|0\rangle$$

$$= \left(\frac{1}{A}\int \frac{dkdq}{(2\pi)^2} \frac{e^{-\omega\sqrt{(\varepsilon-it)^2}+ikx+iqy}}{2\omega}\right)\left(\frac{1}{A}\int \frac{dkdq}{(2\pi)^2} \frac{e^{-\omega\sqrt{(\varepsilon+it)^2}}}{2\omega}\right) + \text{c.c.}, \tag{12}$$

with the overall normalization factor given by

$$\langle \phi(i\varepsilon, 0, 0)\phi(-i\varepsilon, 0, 0)\rangle = \frac{1}{A}\int \frac{dkdq}{(2\pi)^2} \frac{e^{-2\varepsilon\omega}}{2\omega}. \tag{13}$$

The dynamics of the ϕ^2 condensate after the local quench by operator ϕ is given by another type of correlation function, namely,

$$\langle \phi^2(t, x, y)\rangle_\phi = \frac{\langle 0|\phi(i\varepsilon, 0, 0)\phi^2(t, x, y)\phi(-i\varepsilon, 0, 0)|0\rangle}{\langle 0|\phi(i\varepsilon, 0, 0)\phi(-i\varepsilon, 0, 0)|0\rangle}. \tag{14}$$

Objects of this type have been studied in works on operator local quenches [70]. To deal with divergences of composite operator ϕ^2, we split the point at which this operator is inserted into two separate ones, (t_1, x_1) and $(t_2, x_2) = (t_1 + \delta_1, x_1 + \delta_2)$, and take the limit $\delta_{1,2} \to 0$ at the end of the calculation. After that, Wick's contractions are performed, and we obtain

$$\langle \phi^2(t, x, y)\rangle_\phi = \frac{\langle 0|\phi(i\varepsilon, 0, 0)\phi^2(t, x, y)\phi(-i\varepsilon, 0, 0)|0\rangle}{\langle 0|\phi(i\varepsilon, 0, 0)\phi(-i\varepsilon, 0, 0)|0\rangle}$$

$$= \lim_{(t_2, x_2, y_2) \to (t_1, x_1, y_1)} \frac{\langle 0|\phi(i\varepsilon, 0, 0)\phi(t_1, x_1, y_1)\phi(t_2, x_2, y_2)\phi(-i\varepsilon, 0, 0)|0\rangle}{\langle 0|\phi(i\varepsilon, 0, 0)\phi(-i\varepsilon, 0, 0)|0\rangle}$$

$$= 2 \cdot \frac{\langle 0|\phi(i\varepsilon, 0, 0)\phi(t, x, y)|0\rangle\langle 0|\phi(t, x, y)\phi(-i\varepsilon, 0, 0)|0\rangle}{\langle 0|\phi(i\varepsilon, 0, 0)\phi(-i\varepsilon, 0, 0)|0\rangle} + \langle 0|\phi^2(t, x, y)|0\rangle, \tag{15}$$

where the last term is divergent and should be subtracted. We calculate each contraction numerically starting with the two-point function in mixed representation (A6),

$$\langle 0|\phi(i\varepsilon, 0, 0)\phi(t, x, y)|0\rangle\langle 0|\phi(t, x, y)\phi(-i\varepsilon, 0, 0)|0\rangle = \left|\frac{1}{A}\int \frac{dkdq}{(2\pi)^2} \frac{e^{-\omega\sqrt{(\varepsilon-it)^2}+ikx+iqy}}{2\omega}\right|^2. \tag{16}$$
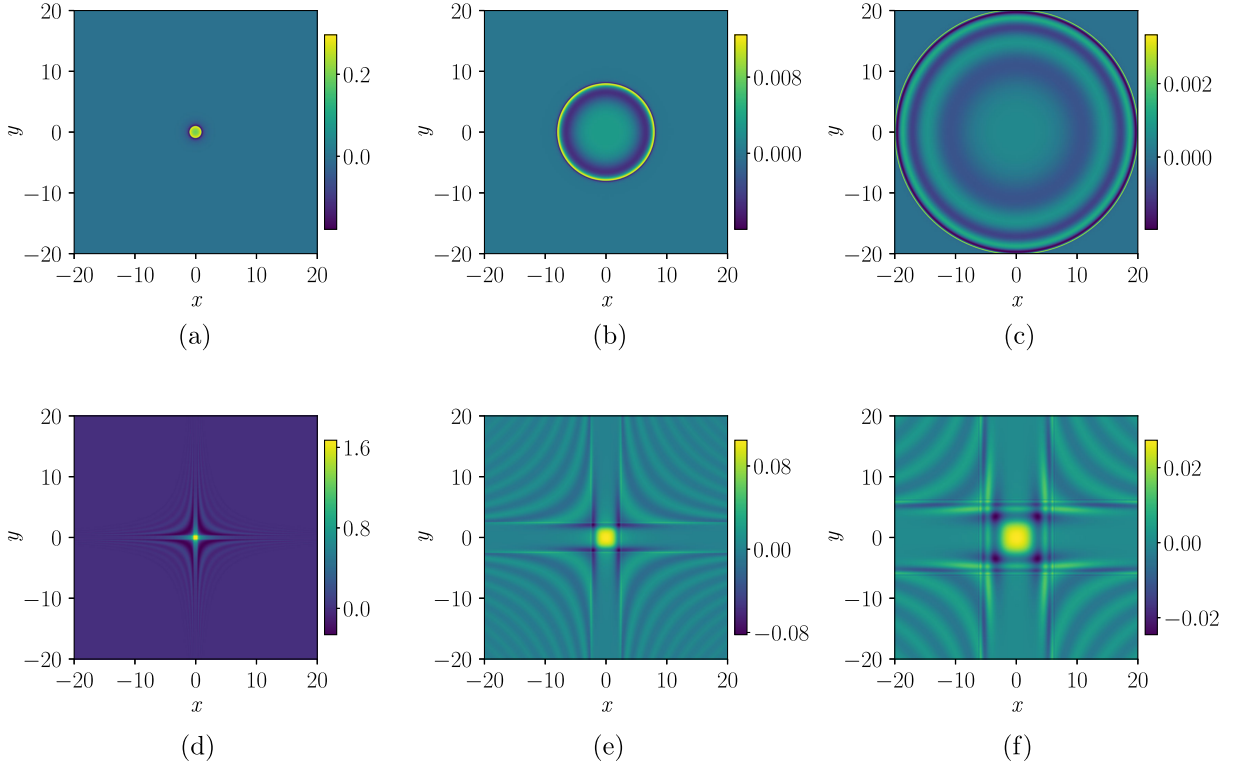
FIG. 1.   Dynamics of the nonequilibrium two-point function after a local quench corresponding to operator ϕ insertion. (a)–(c) Spatial profiles of perturbations for fixed time moments in the relativistic model for $m = 1$, $\varepsilon = 0.05$. (d)–(f) The same for the $\mathbb{Z}_4$-symmetric fractonic model; $m = 1$, $\mu_0 = \mu = 1$, $\varepsilon = 0.05$, $\epsilon = 0.1$. (a) Relativistic, $t = 1$. (b) Relativistic, $t = 8$. (c) Relativistic, $t = 20$. (d) $\mathbb{Z}_4, t = 1$. (e) $\mathbb{Z}_4, t = 8$. (f) $\mathbb{Z}_4, t = 20$.

The numerical results for the postquench dynamics of the relativistic free scalar theory and the fracton field theory are shown in Fig. 1 for the two-point function and in Fig. 2 for the ϕ^2 condensate. One can see that, in the fracton field theory containing the relativistic regulator term, two types of dynamics are present. The severe anisotropy of the fractonic term leads to instantaneous propagation of excitations along the x and y axes, and emergence of wavelike patterns beyond the light cone. On the other hand, the relativistic regulator imposes a speed limit on the propagation of square-shaped wave fronts.

IV. DYNAMICS OF THE ENERGY DENSITY AND DIPOLE MOMENTUM

It is instructive to compare the dynamics of the two-point correlation functions with the propagation of energy density $\mathcal{E}$ given by the following expression,

$$\langle \mathcal{E}(t, x, y) \rangle_\phi = \frac{\langle \phi(i\varepsilon, 0, 0) | \mathcal{E}(t, x, y) | \phi(-i\varepsilon, 0, 0) \rangle}{\langle \phi(i\varepsilon, 0, 0) \phi(-i\varepsilon, 0, 0) \rangle}, \quad (17)$$

where the Euclidean energy density is

$$\mathcal{E} = \frac{1}{2} (-(\partial_\tau \phi)^2 + (\partial_x \phi)^2 + (\partial_y \phi)^2 + m^2 \phi^2) \quad (18)$$

for the relativistic field theory and

$$\mathcal{E} = \frac{1}{2} \left(-\mu_0 (\partial_\tau \phi)^2 + \frac{1}{\mu} (\partial_x \partial_y \phi)^2 + \mu m^2 \phi^2 \right) \quad (19)$$

for the massive fracton scalar field theory (see also Appendix C). Adding the relativistic regulator ϵ to the fractonic theory modifies this expression to

$$\mathcal{E} = \frac{1}{2} \left(-\mu_0 (\partial_\tau \phi)^2 + \epsilon (\partial_x \phi)^2 + \epsilon (\partial_y \phi)^2 \right.$$
$$\left. + \frac{1}{\mu} (\partial_x \partial_y \phi)^2 + \mu m^2 \phi^2 \right). \quad (20)$$

The corresponding numerical results for the postquench dynamics are shown in Fig. 2.

Another observable important in this context is the dipole momentum, since its conservation in time is a characteristic feature of fractonic theories. While, strictly speaking, by introducing the relativistic regularization of the UV/IR mixing we violate the dipole momentum conservation, it is still interesting to look at its dynamics. Specifically, we consider the postquench dynamics of the square of the time component of dipole, given by the following correlation function (see Appendix C for details),
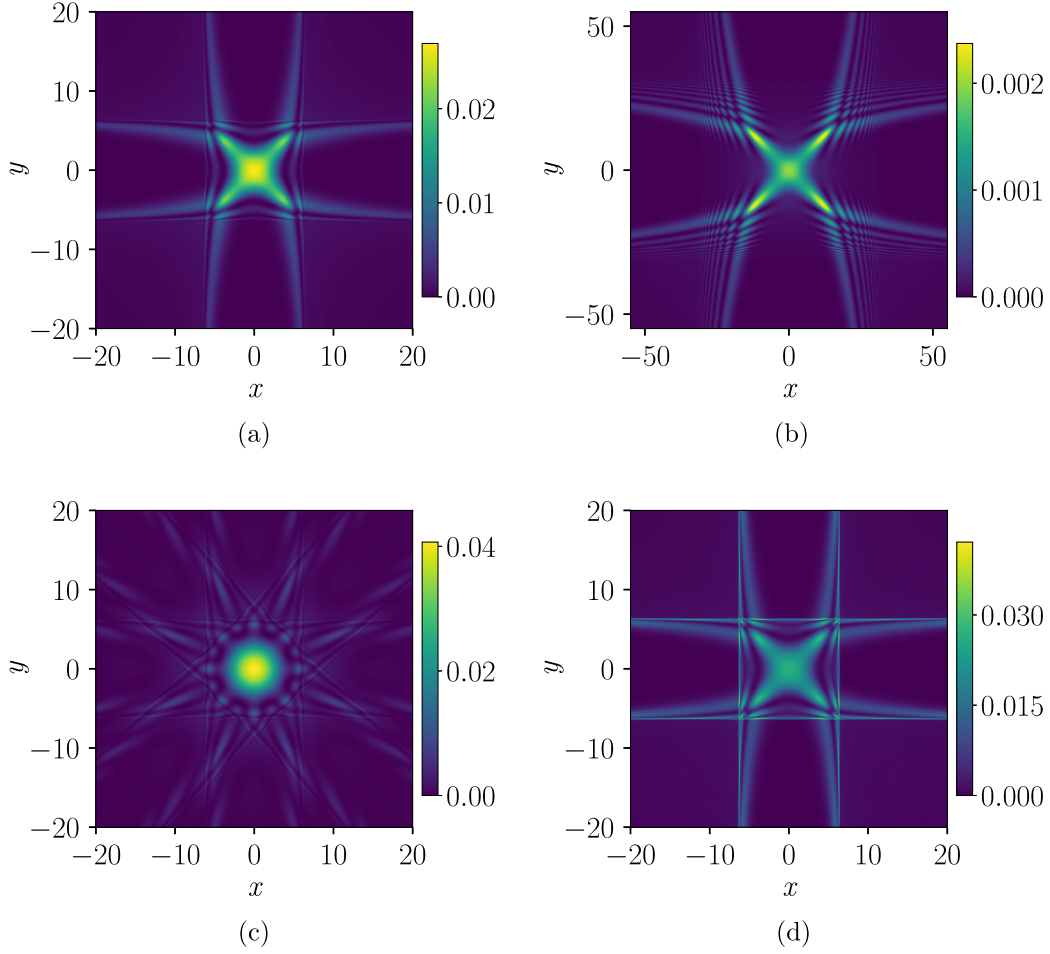
FIG. 2. Dynamics of the observables after a local quench corresponding to insertion of operator ϕ. (a),(b) Spatial profiles of the perturbations of ϕ^2 condensate for fixed moments of time $t = 20$ and $t = 100$ in $\mathbb{Z}_4$-symmetric fractonic model. (c) Spatial profile of the perturbations of ϕ^2 condensate for a fixed moment of time $t = 20$ in $\mathbb{Z}_8$-symmetric fractonic model. (d) Spatial profile of the perturbations of the energy density for a fixed moment of time $t = 20$ in $\mathbb{Z}_4$-symmetric fractonic model. For all cases, $m = 1$, $\varepsilon = 0.05$, $\mu_0 = \mu = 1$, and $\epsilon = 0.1$. (a) $\langle\phi^2\rangle$, $\mathbb{Z}_4$, $t = 20$. (b) $\langle\phi^2\rangle$, $\mathbb{Z}_4$, $t = 100$. (c) $\langle\phi^2\rangle$, $\mathbb{Z}_8$, $t = 20$. (d) $\langle\mathcal{E}\rangle$, $\mathbb{Z}_4$, $t = 20$.

$$\langle J_0^2\rangle = \frac{\langle\phi(i\varepsilon, 0, 0)|J_0^2(t, x, y)|\phi(-i\varepsilon, 0, 0)\rangle}{\langle\phi(i\varepsilon, 0, 0)\phi(-i\varepsilon, 0, 0)\rangle}, \quad (21)$$

where the time component of the dipole current is

$$J_0 = \mu_0\partial_t\phi. \quad (22)$$

In Fig. 3, we show the spatial profile of $\langle J_0^2\rangle$ for $t = 100$. One can see that the general structure is similar to other observables, but a manifold of excitation fronts emerges and leads to a complex interference picture near the corners of the square formed by the wave fronts.

V. INSTANTANEOUS SIGNAL PROPAGATION AND THE LIEB-ROBINSON BOUND

As evident from the postquench evolution profiles shown in the previous sections, a local pointlike
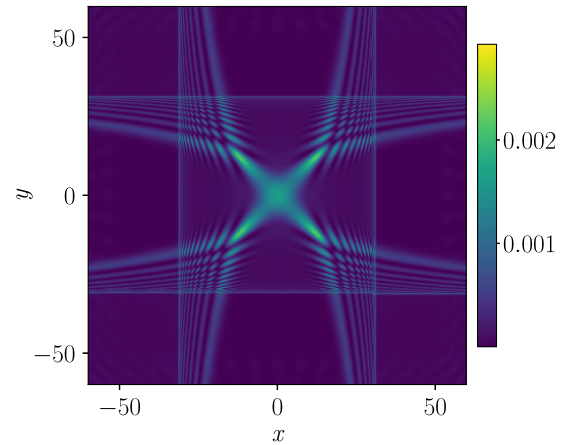

FIG. 3. Spatial profile of $\langle J_0^2\rangle$ after a local quench corresponding to operator ϕ insertion for a fixed moment of time $t = 100$ for $m = 1$, $\varepsilon = 0.05$, $\mu_0 = \mu = 1$, and $\epsilon = 0.1$.

perturbation of fractonic medium instantaneously excites points far away from the perturbation region, violating causality. Adding a relativistic term to the action changes the excitation patterns but does not recover causal dynamics. On the other hand, the fracton field theory can be viewed as a continuum limit of a many-body lattice quantum theory with local interactions, for which the Lieb-Robinson bound setting an effective light cone can be expected to exist. Hence, it is important to analyze this apparent discrepancy and understand whether the Lieb-Robinson bound induces the finite speed of signal propagation in the continuum theory.

First, we briefly remind the reader of the main conditions, which a lattice many-body quantum model should satisfy to ensure the existence of the Lieb-Robinson bound. For that, we shall closely follow Ref. [72]. Let us consider a general harmonic system on lattice $\mathscr{L}$, defined by a Hamiltonian of the form

$$H_N = \frac{1}{2}\left[\sum_{\mathbf{i,j}\in\mathscr{L}} \hat{p}_\mathbf{i} P_{\mathbf{i,j}} \hat{p}_\mathbf{j} + \hat{x}_\mathbf{i} X_{\mathbf{i,j}} \hat{x}_\mathbf{j}\right], \qquad (23)$$

with a locality constraint: $X_{\mathbf{i,j}} = 0$ for $d(\mathbf{i,j}) > R$, where $d(\mathbf{i,j})$ is the length of the shortest path on the lattice between sites $\mathbf{i}$ and $\mathbf{j}$ and R is a fixed constant. For many systems including the discretization of the fracton field theory considered here, $P_{\mathbf{i,j}} = \delta_{\mathbf{i,j}}$, so we shall assume this in the subsequent discussion. Then, introducing rescaled time,

$$\tau \equiv \sqrt{\|X\|}|t|, \qquad (24)$$

one can claim that the Lieb-Robinson bound is satisfied [72],

$$\sqrt{\|X\|}\|[\hat{x}_\mathbf{i}(t), \hat{x}_\mathbf{j}]\| \le \frac{\sqrt{R}e^{2d(\mathbf{i,j})\log\left(\frac{eR\tau}{2d(\mathbf{i,j})}\right)}}{\sqrt{d(\mathbf{i,j})}\left(1 - \left(\frac{eR\tau}{2d(\mathbf{i,j})}\right)^2\right)}$$

$$\text{for } d(\mathbf{i,j}) > eR\tau/2. \qquad (25)$$

In this case, an effective light cone arises, the interior of which is defined as

$$d(\mathbf{i,j}) < c|t| \propto eR\tau/2, \qquad (26)$$

with effective speed of light c given by

$$c \propto \frac{1}{2}eR\sqrt{\|X\|}. \qquad (27)$$

To derive the exact emergent speed of light, more assumptions are required, but it is only important for us whether it is bounded from above or not.

Now, let us construct the discretization of the fracton field theory, which is given in the continuum limit by its Lagrangian density,

$$\mathcal{L} = \frac{\mu_0}{2}(\partial_t\phi)^2 - \frac{1}{2\mu}(\partial_x\partial_y\phi)^2 - \frac{\epsilon}{2}(\partial_x\phi)^2 - \frac{\epsilon}{2}(\partial_y\phi)^2 - \frac{\mu m^2}{2}\phi^2, \qquad (28)$$

where we included the mass term and the relativistic regulator. The corresponding Hamiltonian density is

$$\mathcal{H} = \frac{\mu_0}{2}(\partial_t\phi)^2 + \frac{1}{2\mu}(\partial_x\partial_y\phi)^2 + \frac{\epsilon}{2}(\partial_x\phi)^2 + \frac{\epsilon}{2}(\partial_y\phi)^2 + \frac{\mu m^2}{2}\phi^2. \qquad (29)$$

The derivatives can be discretized as

$$\partial_x\phi \to \frac{1}{1/N}\left[\phi_{i_x+1,i_y} - \phi_{i_x,i_y}\right],$$

$$\partial_y\phi \to \frac{1}{1/N}\left[\phi_{i_x,i_y+1} - \phi_{i_x,i_y}\right],$$

$$\partial_x\partial_y\phi \to \frac{1}{1/N^2}\left[\phi_{i_x+1,i_y+1} - \phi_{i_x+1,i_y} - \phi_{i_x,i_y+1} + \phi_{i_x,i_y}\right], \qquad (30)$$

where we assumed that the system is defined on a square lattice $[0,L] \times [0,L]$, i_x and i_y denote sites, and N^2 is the total number of sites. To simplify consideration, we fix $L = 1$. In contrast with (2.2) in Ref. [8], we introduce here lattice constant $a = 1/N$. On the resulting lattice, it is handy to define finite-difference operators,

$$\Delta_x\phi_{i_x,i_y} \equiv \frac{\phi_{i_x+1,i_y} - \phi_{i_x,i_y}}{1/N},$$

$$\Delta_y\phi_{i_x,i_y} \equiv \frac{\phi_{i_x,i_y+1} - \phi_{i_x,i_y}}{1/N}. \qquad (31)$$

The corresponding discretized Hamiltonian is

$$H_N = \frac{1}{2N^2}\sum_{\{i_x,i_y\}\in\mathscr{L}}\left(\mu_0\pi_{i_x,i_y}^2 + \frac{N^4}{\mu}[\phi_{i_x+1,i_y+1} - \phi_{i_x+1,i_y}\right.$$

$$\left. - \phi_{i_x,i_y+1} + \phi_{i_x,i_y}]^2 + \epsilon N^2[\phi_{i_x+1,i_y} - \phi_{i_x,i_y}]^2 \right.$$

$$\left. + \epsilon N^2[\phi_{i_x,i_y+1} - \phi_{i_x,i_y}]^2 + \mu m^2\phi_{i_x,i_y}^2\right), \qquad (32)$$

where π is the canonical momentum operator. After some transformations, it acquires the following form,

$$H_N = \frac{\mu_0}{2N^2} \sum_{\{i_x,i_y\},\{j_x,j_y\} \in \mathscr{L}} \left(\pi_{i_x,i_y} \delta_{i_x,j_x} \delta_{i_y,j_y} \pi_{j_x,j_y} \right.$$

$$+ \frac{N^4}{\mu\mu_0} \left[\left(4 + \frac{4\mu\epsilon}{N^2} + \frac{\mu^2 m^2}{N^4} \right) \phi_{i_x,i_y} \delta_{i_x,j_x} \delta_{i_y,j_y} \phi_{j_x,j_y} \right.$$

$$- \left(2 + \frac{\mu\epsilon}{N^2} \right) \phi_{i_x,i_y} \delta_{i_x,j_x} \delta_{i_y,j_y} (\tilde{\Delta}_x + \tilde{\Delta}_y) \phi_{j_x,j_y}$$

$$\left. \left. + \phi_{i_x,i_y} \delta_{i_x,j_x} \delta_{i_y,j_y} \tilde{\Delta}_{x,y} \phi_{j_x,j_y} \right] \right), \tag{33}$$

where we defined lattice operators $\tilde{\Delta}$ as

$$\tilde{\Delta}_x \phi_{i_x,i_y} \equiv \phi_{i_x+1,i_y} + \phi_{i_x-1,i_y},$$

$$\tilde{\Delta}_y \phi_{i_x,i_y} \equiv \phi_{i_x,i_y+1} + \phi_{i_x,i_y-1},$$

$$\tilde{\Delta}_{x,y} \phi_{i_x,i_y} \equiv \phi_{i_x+1,i_y+1} + \phi_{i_x-1,i_y+1} + \phi_{i_x+1,i_y-1} + \phi_{i_x-1,i_y-1}. \tag{34}$$

In the intermediate calculation, we used the translational invariance and reshuffled the indices.

Introducing shorthand notations, $\delta_{\mathbf{i},\mathbf{j}} \equiv \delta_{i_x,j_x} \delta_{i_y,j_y}$, $\phi_{\mathbf{i}} \equiv \phi_{i_x,i_y}$, and redefining coordinate (field) and momentum operators as

$$\hat{x}_{\mathbf{i}} \equiv N^{-1} \phi_{\mathbf{i}},$$

$$\hat{p}_{\mathbf{i}} \equiv N^{-1} \pi_{\mathbf{i}}, \tag{35}$$

we can rewrite the Hamiltonian in the conventional harmonic form,

$$H_N = \frac{\mu_0}{2} \left[\sum_{\mathbf{i},\mathbf{j} \in \mathscr{L}} \hat{p}_{\mathbf{i}} P_{\mathbf{i},\mathbf{j}} \hat{p}_{\mathbf{j}} + \hat{x}_{\mathbf{i}} X_{\mathbf{i},\mathbf{j}} \hat{x}_{\mathbf{j}} \right], \tag{36}$$

with $P_{\mathbf{i},\mathbf{j}} = \delta_{\mathbf{i},\mathbf{j}}$ and $X_{\mathbf{i},\mathbf{j}} = X \delta_{\mathbf{i},\mathbf{j}}$, where

$$X = \frac{N^4}{\mu\mu_0} \left[f(N,\mu,\epsilon) - g(N,\mu,\epsilon)(\tilde{\Delta}_x + \tilde{\Delta}_y) + \tilde{\Delta}_{x,y} \right], \tag{37}$$

and

$$f(N,\mu,\epsilon) = 4 + \frac{4\mu\epsilon}{N^2} + \frac{\mu^2 m^2}{N^4},$$

$$g(N,\mu,\epsilon) = 2 + \frac{\mu\epsilon}{N^2}. \tag{38}$$

To get a bound on the norm $\|X\|$, we first obtain spectrum of this matrix. Through a direct substitution, it can be shown that any plane wave is an eigenfunction of X,

$$\sum_{\mathbf{j} \in \mathscr{L}} X_{\mathbf{i},\mathbf{j}} \exp\left(\frac{2\pi i}{N} \mathbf{k} \cdot \mathbf{j} \right) = \lambda_{\mathbf{k}} \exp\left(\frac{2\pi i}{N} \mathbf{k} \cdot \mathbf{i} \right), \tag{39}$$

where $\mathbf{k} = (k_x, k_y)$ and k_x, k_y, i_x, i_y, j_x, j_y take integer values from 0 to $N-1$, with the eigenvalues

$$\lambda_{\mathbf{k}} = \frac{16N^4}{\mu\mu_0} \sin^2\left(\frac{\pi k_x}{N} \right) \sin^2\left(\frac{\pi k_y}{N} \right)$$

$$+ \frac{4N^2\epsilon}{\mu_0} \left(\sin^2\left(\frac{\pi k_x}{N} \right) + \sin^2\left(\frac{\pi k_y}{N} \right) \right) + \frac{\mu m^2}{\mu_0}. \tag{40}$$

We shall show that the emergent speed of light in the fractonic theory can be unbounded from above. Let us pick a particular norm, $\|X\| = \|X\|_2$, namely, the spectral norm, in (27). Then, the following identity holds:

$$\|X\|_2 = |\lambda|_{\max}. \tag{41}$$

Here, the critical difference between the fractonic theory and the relativistic theory becomes clear. First, let us assume that the dispersion relation contains only the relativistic and massive terms, but not the fractonic part, and take for simplicity $\mu = \mu_0 = \epsilon = 1$. Then,

$$\|X\|_2 = 8N^2 + m^2, \tag{42}$$

and in the continuum limit, one obtains

$$c \propto \frac{1}{2} eR\sqrt{\|X\|_2} = \frac{1}{2} \cdot e \cdot \frac{2}{N} \sqrt{8N^2 + m^2} \to 2\sqrt{2}e,$$

$$\text{as } N \to \infty. \tag{43}$$

On the other hand, in the discrete version of the fractonic theory, the leading term in the dispersion relation scales as $\sim N^4$; hence, in the continuum limit, $R\sqrt{\|X\|_2} \sim N \to \infty$.

At this point, it is only an indication of the fact that there is no continuum limit of the Lieb-Robinson bound in fracton systems, because in the lhs of (25) there is also commutator $\|[\hat{x}_{\mathbf{i}}(t), \hat{x}_{\mathbf{j}}]\|$, which can in principle compensate for the rapid growth of $\sqrt{\|X\|}$. Hence, we need to analyze it as well.

For that, we rely on (56) from Ref. [72]. If $P_{\mathbf{i},\mathbf{j}} \propto \delta_{\mathbf{i},\mathbf{j}}$, the commutator of position operators at different times in the harmonic theory can be represented as a series

$$C_{\mathbf{i},\mathbf{j}}^{xx}(t) \equiv i[\hat{x}_{\mathbf{i}}(t), \hat{x}_{\mathbf{j}}] = \sum_{n=0}^{\infty} \frac{(-1)^n t^{2n+1} (X^n)_{\mathbf{i},\mathbf{j}}}{(2n+1)!}, \tag{44}$$

that boils down to matrix-valued function

$$C^{xx}(t) = \frac{\sin(t\sqrt{X})}{\sqrt{X}}. \tag{45}$$

It can be evaluated in the diagonal basis of X in the momentum space and then Fourier transformed back to the coordinate representation:

$$C_{\mathbf{i},\mathbf{j}}^{xx}(t) = \frac{1}{N^2}\sum_{\mathbf{k}} \frac{\sin(t\sqrt{\lambda_{\mathbf{k}}})}{\sqrt{\lambda_{\mathbf{k}}}}\exp\left(\frac{2\pi i}{N}(\mathbf{k}\cdot\mathbf{i}-\mathbf{k}\cdot\mathbf{j})\right). \quad (46)$$

Prefactor N^{-2} here comes from inversion of the basis vectors.

In the continuum limit, we should rather consider the commutator of field operators

$$[\phi_{\mathbf{i}}(t), \phi_{\mathbf{j}}] = N^2[\hat{x}_{\mathbf{i}}(t), \hat{x}_{\mathbf{j}}], \quad (47)$$

which we denote as $\tilde{C}_{\mathbf{i},\mathbf{j}}^{xx}(t) = N^2 C_{\mathbf{i},\mathbf{j}}^{xx}(t)$.

The apparent superluminal signal propagation occurs along the symmetry lines of the fractonic theory, so it is sufficient to analyze behavior of the commutator along one of the coordinate axes. Specifically, we can pick up two points lying on the y axis, $\mathbf{i} = \mathbf{i}_0 = \mathbf{0}$ and $\mathbf{j} = \mathbf{j}_r = (0, rN)$, with $rN \in \mathbb{Z}$, which turn into $(0,0)$ and $(0, r)$ in the continuum limit. Then,

$$\tilde{C}_{\mathbf{i}_0,\mathbf{j}_r}^{xx}(t) = \sum_{\mathbf{k}} \frac{\sin(t\sqrt{\lambda_{\mathbf{k}}})}{\sqrt{\lambda_{\mathbf{k}}}} e^{-2\pi i r k_y}. \quad (48)$$

In the case of the nonregularized fractonic theory with $m = 0$ and $\epsilon = 0$, we can proceed by splitting the sum into three parts: summation over points with momenta $(k_x, 0)$, summation over points with momenta $(0, k_y)$ (for these two groups $\lambda_{\mathbf{k}} = 0$), and summation over other points ($k_x > 0$, $k_y > 0$). We get

$$\tilde{C}_{\mathbf{i}_0,\mathbf{j}_r}^{xx}(t) = tN + t\sum_{k_y=1}^{N-1} e^{-2\pi i r k_y} + \sum_{k_x,k_y=1}^{N-1} \frac{\sin(t\sqrt{\lambda_{\mathbf{k}}})}{\sqrt{\lambda_{\mathbf{k}}}} e^{-2\pi i r k_y}. \quad (49)$$

The next step is to find an upper bound on the last sum in (49),

$$\left|\sum_{k_x,k_y=1}^{N-1} \frac{\sin(t\sqrt{\lambda_{\mathbf{k}}})}{\sqrt{\lambda_{\mathbf{k}}}} e^{-2\pi i r k_y}\right|$$
$$\leq \sum_{k_x,k_y=1}^{N-1} \frac{|\sin(t\sqrt{\lambda_{\mathbf{k}}})|}{|\sqrt{\lambda_{\mathbf{k}}}|}|e^{-2\pi i r k_y}| \leq \sum_{k_x,k_y=1}^{N-1} \frac{1}{|\sqrt{\lambda_{\mathbf{k}}}|}. \quad (50)$$

Recalling (40), the fact that $\sin x > x/2$ for $x \in (0, \pi/2)$, and the symmetry $\sin\alpha = \sin(\pi - \alpha)$, one can obtain the following estimate,

$$\sum_{k_x,k_y=1}^{N-1} \frac{1}{|\sqrt{\lambda_{\mathbf{k}}}|} \leq \frac{\sqrt{\mu\mu_0}}{\pi^2} \sum_{k_x,k_y=1}^{\lfloor\frac{N}{2}\rfloor} \frac{1}{k_x k_y}, \quad (51)$$

where $\lfloor\frac{N}{2}\rfloor$ denotes the integer part of the fraction. The resulting sum can be estimated from above by integral

$$\sum_{k_x,k_y=1}^{\lfloor\frac{N}{2}\rfloor} \frac{1}{k_x k_y} = \left(\sum_{k=1}^{\lfloor\frac{N}{2}\rfloor} \frac{1}{k}\right)^2 \leq \left(1 + \int_1^{\lfloor\frac{N}{2}\rfloor+1} \frac{du}{u}\right)^2$$
$$= \left(1 + \ln\left(\lfloor\frac{N}{2}\rfloor + 1\right)\right)^2. \quad (52)$$

The second term of (49) is

$$t\sum_{k_y=1}^{N-1} e^{-2\pi i r k_y} = t\left(-1 + \frac{e^{-2\pi i r N} - 1}{e^{-2\pi i r} - 1}\right), \quad (53)$$

and for any $r \in (0, 1)$,

$$\left|\frac{e^{-2\pi i r N} - 1}{e^{-2\pi i r} - 1}\right| \leq \frac{2}{|e^{-2\pi i r} - 1|}. \quad (54)$$

Now, using the fact that, if $a = b + c + d$ and $|c| \leq f$, $|d| \leq g$, then $a \geq b - f - g$, one can derive the following lower bound on the commutator:

$$\left|\tilde{C}_{\mathbf{i}_0,\mathbf{j}_r}^{xx}(t)\right| \geq t(N-1) - \frac{2t}{|e^{-2\pi i r} - 1|}$$
$$- \frac{\sqrt{\mu\mu_0}}{\pi^2}\left(1 + \ln\left(\lfloor\frac{N}{2}\rfloor + 1\right)\right)^2. \quad (55)$$

Since the linear term grows faster than the logarithmic one, the norm of the commutator is divergent for large N, for any distances along the cross $x = 0$ and $y = 0$ and any values of time except $t = 0$. Hence, lhs of (25), which in the continuum case takes the form $\sqrt{\|X\|}\|[\phi_{\mathbf{i}}(t), \phi_{\mathbf{j}}]\|$, is a product of two terms unbounded from above, and the Lieb-Robinson bound is satisfied only for smaller and smaller values of times t as the lattice spacing goes to zero. As a result, in the continuum limit, the effective speed of light in the fractonic theory can be unbounded.

This calculation also explains why introducing the massive term and the relativistic regulator does not remove the noncausal signal propagation. In the expression for eigenvalues (40), these terms scale slower with N than the fractonic term and hence cannot compensate for the unlimited growth of $\|X\|$ and $\|[\phi_{\mathbf{i}}(t), \phi_{\mathbf{j}}]\|$ in the continuum limit.

VI. LOCAL QUENCH IN FINITE VOLUME

The norm of a state locally perturbed by an operator in a theory defined on a plane is infinite. Hence, it is instructive to study postquench dynamics in a regularized theory, where the norm divergence is removed by putting the system on a finite torus. Here, we consider the evolution of observables after a local quench with operator ϕ on a $2 + 1$-dimensional Lorentzian torus, i.e., $x \sim x + L_x$, $y \sim y + L_y$. Starting with the general form of the two-point function (refer to (B5) in Appendix B), nonequilibrium Green's function $G(t, x, y)$ (10) is calculated via the following Wick's contractions,

$$\langle\phi(i\varepsilon,0,0)\phi(t,x,y)\rangle\langle\phi(t,0,0)\phi(-i\varepsilon,0,0)\rangle + \langle\phi(i\varepsilon,0,0)\phi(t,0,0)\rangle\langle\phi(t,x,y)\phi(-i\varepsilon,0,0)\rangle$$

$$= \left(\frac{1}{AL_xL_y}\cdot\frac{e^{-m\sqrt{(\varepsilon-it)^2}}}{2m} + \frac{1}{AL_xL_y}\sum_{n,s\neq 0}e^{ik_nx+iq_sy}\left(\frac{e^{-\omega_{ns}\sqrt{(\varepsilon-it)^2}}}{2\omega_{ns}}\right)\right)$$

$$\times \left(\frac{1}{AL_xL_y}\cdot\frac{e^{-m\sqrt{(\varepsilon+it)^2}}}{2m} + \frac{1}{AL_xL_y}\sum_{n,s\neq 0}\frac{e^{-\omega_{ns}\sqrt{(\varepsilon+it)^2}}}{2\omega_{ns}}\right) + \text{c.c.,} \tag{56}$$

and the correlation function of ϕ^2 condensate $\langle\phi^2\rangle_\phi$ (14),

$$\langle\phi(i\varepsilon,0,0)\phi(t,x,y)\rangle\langle\phi(t,x,y)\phi(-i\varepsilon,0,0)\rangle = \left|\frac{1}{AL_xL_y}\cdot\frac{e^{-m\sqrt{(\varepsilon-it)^2}}}{2m} + \frac{1}{AL_xL_y}\sum_{n,s\neq 0}e^{ik_nx+iq_sy}\left(\frac{e^{-\omega_{ns}\sqrt{(\varepsilon-it)^2}}}{2\omega_{ns}}\right)\right|^2 \tag{57}$$

with the normalization factor

$$N = \langle\phi(i\varepsilon,0,0)\phi(-i\varepsilon,0,0)\rangle$$
$$= \frac{1}{AL_xL_y}\cdot\frac{e^{-2m\varepsilon}}{2m} + \frac{1}{AL_xL_y}\sum_{n,s\neq 0}\frac{e^{-2\omega_{ns}\varepsilon}}{2\omega_{ns}}. \tag{58}$$

The sums over Fourier modes will be calculated numerically.

As a warm-up, we first consider the evolution of ϕ^2 condensate in the Klein-Gordon massive free theory. Note that the massless limit $m \to 0$ of the two-point function (B5) does not exist. This is a general result for any number of compact dimensions since the divergent term $e^{-m\sqrt{\tau^2}}/m$ in the series does not depend on d. However, in the flat-space limit $L_{x,y} \to \infty$, this divergence vanishes, and the two-point function becomes well defined. Both massless and massive flat-space limits $L_{x,y} \to \infty$ can be obtained analytically. For $d = 2+1$, we showed in Ref. [70] that

$$\langle\phi^2(t,x,y)\rangle_{\phi,3d}\underset{L_x,L_y\to\infty}{\approx}\frac{4\varepsilon e^{2\varepsilon m}\left|e^{-m\sqrt{(\varepsilon-it)^2+\rho^2}}\right|^2}{\left|\sqrt{(\varepsilon-it)^2+\rho^2}\right|^2},$$

where $\rho^2 = x^2 + y^2$. \hfill (59)

In contrast with the local quench in CFT$_2$ [38], after which the perturbation propagates as a solitonlike wave and does not dissipate, in $d = 2+1$ dimensions ($d > 2$ in general; see Ref. [70]), the amplitude of the perturbation (59) decays even in the massless limit.

The numerical results for the postquench dynamics are shown in Fig. 4, for the two-point function, and in Fig. 5, for the ϕ^2 condensate. Interestingly, the spatial profiles of correlation functions have highly irregular fractal-looking structures, Figs. 4(c)–4(i). In the case of relativistic field

theory, Fig. 4(c), they appear at larger times simply due to self-interference of the propagating wave front after it circumvents the torus several times. However, for fractons, it is more than that. Naively, one can expect that it is a similar self-interference effect because the noncausally propagating excitations instantaneously wind around the torus for infinitely many times and can interfere immediately. At the same time, as one can see from, e.g., Fig. 4(d), the set of equidistant parallel lines cannot be viewed as a periodic continuation of the original "cross-shaped" excitation across the boundary. These patterns are intricately connected with mathematical properties of sums like (B5) similar to those arising in the description of the Talbot effect in optics [73].

VII. FRACTIONAL DIMENSION OF THE WAVE FRONTS

As is clear from Figs. 4 and 5, evolution of the fractonic model results in rather complicated irregular spatial distributions of the observable values immediately after the quench and, as we discussed above, goes beyond the self-interference effect in contrast with the conventional relativistic model, where highly oscillating patterns emerge at larger times, after the wave front circumvents the torus and interferes with itself. What is interesting to note is that the spatial profiles of $\langle\phi(t,x,y)\phi(0)\rangle$ and $\langle\phi^2(t,x,y)\rangle$ in the fractonic theory are not just highly oscillating but exhibit multiscale self-similarity, i.e., can be regarded as fractals. To show that, we resort to studying fractional dimensions of one-dimensional sections of the two-dimensional patterns using the method suggested in Ref. [74] and previously used by us in Ref. [75]. To perform the case study, we focus on the evolution of $\langle\phi^2(t,x,y)\rangle$, and for each value of t, we take one-dimensional section of the function profile along the $x = y$ line. For the sake of completeness, we provide a brief explanation of the method here.
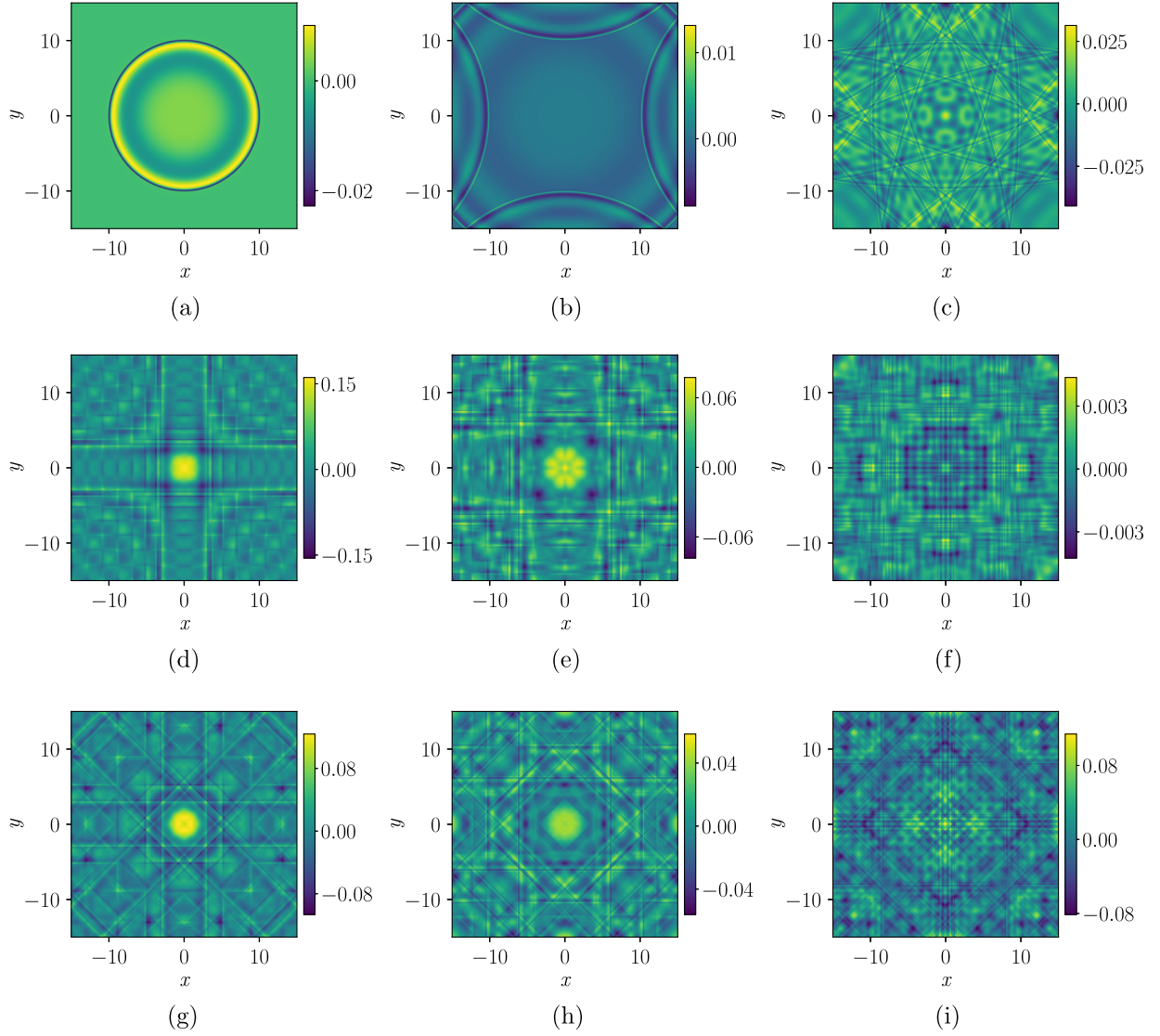
FIG. 4. Dynamics of the nonequilibrium two-point function after a local quench corresponding to the insertion of operator ϕ. (a)–(c) Spatial distribution of perturbations for fixed moments of time in the relativistic model. The parameters are $L_x = L_y = 30$, $m = 1$, and $\varepsilon = 0.05$. (d)–(f) The same for the $\mathbb{Z}_4$-symmetric fractonic model; $L_x = L_y = 30$, $m = 1$, $\varepsilon = 0.05$, $\mu_0 = \mu = 1$, and $\epsilon = 0.1$. (g)–(i) The same for the $\mathbb{Z}_8$-symmetric fractonic model; $L_x = L_y = 30$, $m = 1$, $\varepsilon = 0.05$, $\mu_0 = \mu = 1$, and $\epsilon = 0.1$. (a) Relativistic, $t = 10$. (b) Relativistic, $t = 20$. (c) Relativistic, $t = 100$. (d) $\mathbb{Z}_4, t = 10$. (e) $\mathbb{Z}_4, t = 20$. (f) $\mathbb{Z}_4, t = 100$. (g) $\mathbb{Z}_8, t = 10$. (h) $\mathbb{Z}_8, t = 20$. (i) $\mathbb{Z}_8, t = 100$.

To compute fractional dimension of a one-dimensional profile $\mathcal{O}(x) \equiv \langle \phi^2(t_0, x, x) \rangle$, where coordinate x and value $\mathcal{O}$ have different geometric meanings, the conventional box-counting algorithm cannot be applied. According to Ref. [74], the profile needs to be represented as a discrete set of values $\{\mathcal{O}_i\}$ of length N (in our simulations, we discretize it into $N = 5000$ points). Then, for some integer δ, functions returning the maximal and the minimal values of the set within the δ neighborhood of the ith element of the set are defined as

$$u_\delta(i) = \sup_{i' \in R_\delta(i)} S_{i'},$$

$$b_\delta(i) = \inf_{i' \in R_\delta(i)} S_{i'}, \tag{60}$$

where $R_\delta(i) = \{i' : |i' - i| \le \delta, i' \in [1, N]\}$, and periodic boundary conditions on the set of indices are assumed; $u_\delta(i)$ and $b_\delta(i)$ are the upper and the lower enveloping curves of $\{\mathcal{O}_i\}$. Then, an analog of the box-counting function is defined as
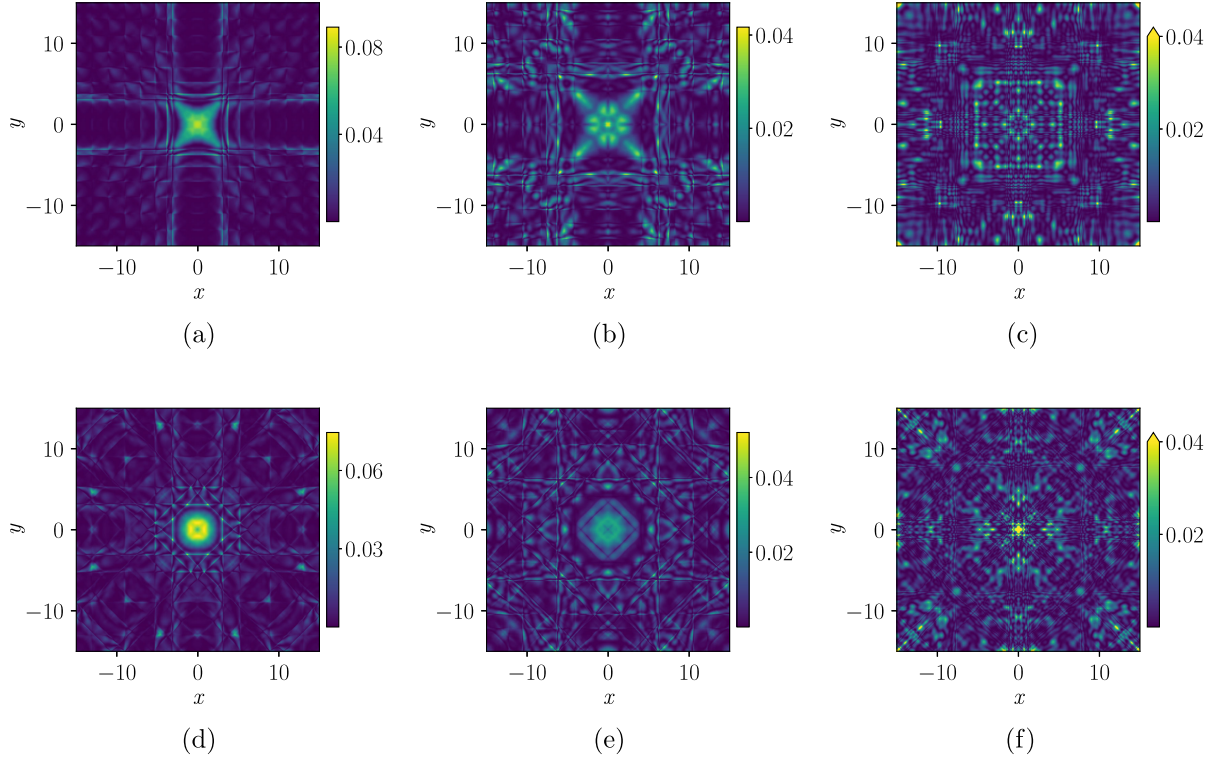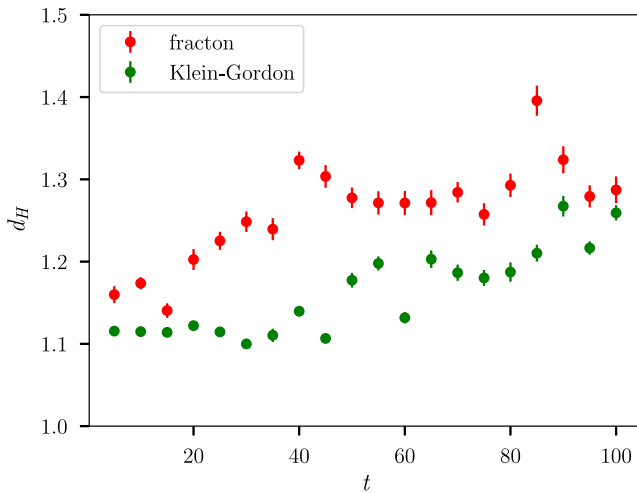
FIG. 5. Dynamics of the ϕ^2 condensate after a local quench corresponding to the insertion of operator ϕ. (a)–(c) Spatial distribution of perturbations for fixed moments of time in the $\mathbb{Z}_4$-symmetric fractonic model. (d)–(f) The same for the $\mathbb{Z}_8$-symmetric fractonic model. For all cases, $L_x = L_y = 30$, $m = 1$, $\varepsilon = 0.05$, $\mu_0 = \mu = 1$, and $\epsilon = 0.1$. (a) $\mathbb{Z}_4, t = 10$. (b) $\mathbb{Z}_4, t = 20$. (c) $\mathbb{Z}_4, t = 100$. (d) $\mathbb{Z}_8, t = 10$. (e) $\mathbb{Z}_8, t = 20$. (f) $\mathbb{Z}_8, t = 100$.

FIG. 6. Fractional dimension of the one-dimensional $x = y$ section of $\langle \phi(t, x, y)^2 \rangle$ profile as a function of time for the fractonic and the relativistic theories. The parameters are $L_x = L_y = 30$, $m = 1$, and $\varepsilon = 0.02$ for both cases and $\mu_0 = \mu = 1$ and $\epsilon = 0.1$ for the fractonic case.
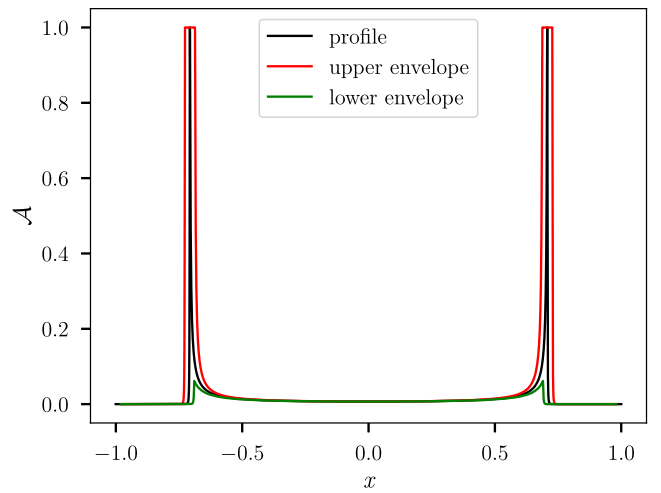
FIG. 7. Upper (red) and lower (green) envelops of a smooth, though peaked, sample curve (black) with amplitude profile $A(x)$ for $\delta = 40$ (5000 points in total). The nonvanishing value of $V(\delta)$ between the envelopes contributes to the fractional dimension estimated by (62).
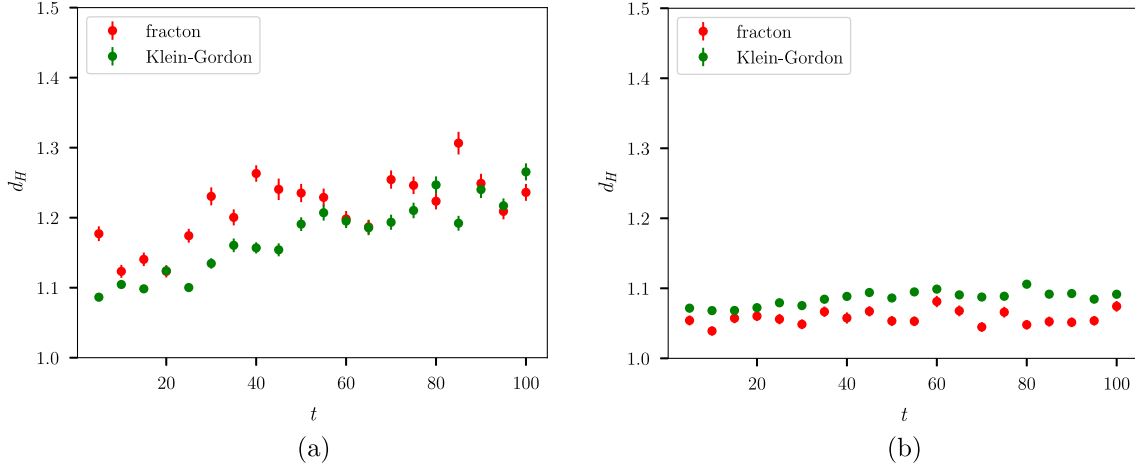
FIG. 8.   Fractional dimension of the one-dimensional $x = y$ section of the two-point function profile as a function of time for the fractonic and the relativistic theories in the cases of the local (a) and global (b) quench. The parameters are (a) $L_x = L_y = 30$, $m = 1$, and $\varepsilon = 0.02$ and (b) slab width $\tau_0 = 0.01$ for both the relativistic and fractonic cases and $\mu_0 = \mu = 1$ and $\epsilon = 0.1$ for the fractonic case.

$$V(\delta) = \frac{1}{\delta^2} \sum_i (u_\delta(i) - b_\delta(i)). \qquad (61)$$

It returns the number of $\delta \times \delta$ blocks within the band between $u_\delta(i)$ and $b_\delta(i)$ envelopes. The fractional dimension d_H is then obtained by fitting this function with a power-law

$$V(\delta) = \frac{a}{\delta^{d_H}}. \qquad (62)$$

It is worth noticing that the scaling is never perfectly algebraic, but the resulting fit errors are rather small. To estimate d_H, we make fit of $V(\delta)$ for a range $\delta \in [2, 80]$. The result for d_H of the one-dimensional sections of $\langle \phi^2 \rangle$ as a function of t is shown in Fig. 6.

It should be noted that this method tends to overestimate the fractional dimension and gives $d_H \simeq 1.1$ for regular nonfractal curves with a few sharp peaks as in Fig. 7 (a typical example of this is the profiles of excitations in the relativistic theory at small times). This artifact is unavoidable when the Hausdorff dimension is estimated numerically. If the δ value is larger than the characteristic width of the peak, the difference between the upper and the lower envelopes is non-negligible and contributes to (62) shifting d_H from 1. By taking this into account, we can see from Fig. 6 that the Hausdorff dimension of the wave front in relativistic field theory acquires nontrivial values after a certain period of time, when the signal circumvents the torus and self-interferes. For the fracton field theory, the dimension is rather high from the very beginning and always exceeds that of the relativistic wave front.

Remarkably, it is the analysis of fractional dimensions that allows us to make a comparison between the local quench setup of this paper and the simpler setup of global quench in fractonic theories, which was investigated in Ref. [25]. In that setup, the system is taken out of equilibrium by abrupt change of the parameters or the symmetries of the system. Since the excitation is global, one-point correlation functions depend trivially on spatial coordinates. Hence, we should compare two-point function instead of $\langle \phi^2(t, x, y) \rangle$ correlator. In Fig. 8, we plotted the corresponding dependencies. In the local quench setup, the fractonic theory fractional dimension still grows faster than in the relativistic theory, although the difference is now less pronounced. The global quench setup (here, the boundary global quench, which is characterized by the slab width) comes as the complete opposite: not only do fractional dimensions both for the fractonic and the relativistic cases hardly grow, but even the dimension in the fractonic case lies lower than for the relativistic one.

This hints to us that, even if the dynamics of two systems look quite similar in their irregular character, the systems may demonstrate different behavior of the features characterizing this irregularity.[3]

VIII. CONCLUSIONS

We have analyzed the out-of-equilibrium dynamics following a local pointlike quench in fracton field theories, and, rather expectedly, it turns out to be very distinct from that of conventional relativistic quantum fields. While in the relativistic settings the initially localized excitation

---

[3]For more on this issue, refer to an upcoming paper [76].

propagates outward continuously delocalizing, in free fractonic theory, the very notion of local quench is somewhat questionable: due to the strong UV/IR mixing, a pointlike perturbation instantaneously excites the system along the lines of discrete symmetry of the theory, creating a nonlocal pattern of correlations in no time. This observation is supported by the fact that the Lieb-Robinson bound for fractonic theories degenerates along the mobility directions in the continuum limit and no longer imposes causality constraints. By introducing mass and the relativistic regularization term, it is possible to induce causal dynamics of wave fronts in the fractonic theory; however, the noncausal instantaneous propagation of signals does not go away, and these two coexist, leading to nontrivial interference patterns. It should be noted that mass and the relativistic regularizaion violate the dipole momentum conservation law—the defining feature of fractons—but still allow one to obtain a tractable approximate story of what happens during the strongly singular and UV/IR mixed dynamics of the non-regularized theory. In particular, the postquench dynamics in fracton field theories preserves the $\mathbb{Z}_n$ symmetry of the theory, as can be seen from the geometry of causal wave fronts. When the free fracton field is placed in a finite volume, fractal-like patterns of excitations emerge across the whole space immediately after the quench. This effect is observed only for locally introduced perturbation, not for the global (as in Ref. [25]) one and goes beyond self-interference of noncausally propagating signals requiring further investigations.

A few questions arise from these considerations. First of all, while the fractonic theories by definition violate the Lorentz symmetry, the fact that they do it in a way that results in noncausal signal propagation is undesirable. Finding a modification of the fractonic model that has a strict propagation speed limit is an important problem. Studying out-of-equilibrium dynamics in an interacting fracton field theory can potentially shed light on this issue. Along the same lines, it is interesting to more deeply understand the connection between noncausal propagation and the emergence of fractal excitation patterns. While it is tempting to relate these two aspects, the fact that the interference of instantaneously propagating signal alone cannot explain these structures leads to a question of if this effect persists in modifications of fracton field theories with restored causality.

ACKNOWLEDGMENTS

APPENDIX A: FRACTONIC PROPAGATOR ON A TWO-DIMENSIONAL PLANE

The action of the Euclidean free massive fracton field theory [8,10] with the relativistic regularization [25] is given by (7). The corresponding equation of motion reads

$$-\mu_0\ddot{\phi} - \epsilon(\partial_x^2\phi + \partial_y^2\phi) + \frac{1}{\mu}\partial_x^2\partial_y^2\phi + \mu m^2\phi = 0. \quad \text{(A1)}$$

In momentum space, it takes the form

$$\left(\mu_0\omega^2 + \epsilon(k^2 + q^2) + \frac{k^2q^2}{\mu} + \mu m^2\right)\phi = 0, \quad \text{(A2)}$$

and the corresponding dispersion relation of the theory is

$$\omega^2(k, q) = -\frac{1}{\mu_0\mu}(\epsilon\mu(k^2 + q^2) + k^2q^2 + \mu^2m^2). \quad \text{(A3)}$$

The Euclidean two-point function of the massive scalar fractonic field (A1) is given by the Fourier transform

$$\langle\phi(\tau,x,y)\phi(0,0,0)\rangle = \frac{1}{A}\mathcal{F}_{\omega,k,q}\left[\frac{\mu}{\mu_0\mu\omega^2 + \epsilon\mu(k^2+q^2) + k^2q^2 + \mu^2m^2}\right]$$

$$\equiv \frac{1}{A}\int\frac{d\omega dk dq}{(2\pi)^3}\frac{\mu e^{i\omega\tau+ikx+iqy}}{\mu_0\mu\omega^2 + \epsilon\mu(k^2+q^2) + k^2q^2 + \mu^2m^2}. \tag{A4}$$

The Fourier transformation with respect to ω gives

$$\mathcal{F}_\omega\left[\frac{\mu}{\mu_0\mu\omega^2 + \epsilon\mu(k^2+q^2) + k^2q^2 + \mu^2m^2}\right] = \frac{1}{2\mu_0}\sqrt{\frac{\mu_0\mu}{\epsilon\mu(k^2+q^2) + k^2q^2 + \mu^2m^2}}$$

$$\times\exp\left[-|\tau|\sqrt{\frac{\epsilon\mu(k^2+q^2) + k^2q^2 + \mu^2m^2}{\mu_0\mu}}\right]. \tag{A5}$$

The other two transformations with respect to k and q cannot be calculated analytically, so we leave the correlation function in the mixed representation with explicit dependence on x and y coordinates,

$$\langle\phi(\tau,x,y)\phi(0,0,0)\rangle = \frac{1}{2A\mu_0}\int\frac{dk dq}{(2\pi)^2}\sqrt{\frac{\mu_0\mu}{\epsilon\mu(k^2+q^2) + k^2q^2 + \mu^2m^2}}e^{-\sqrt{\tau^2}\sqrt{\frac{\epsilon\mu(k^2+q^2)+k^2q^2+\mu^2m^2}{\mu_0\mu}}+ikx+iqy}. \tag{A6}$$

Note that we substituted $|\tau|$ with $\sqrt{\tau^2}$ in the final expression in order to make clear how to perform analytical continuation to the Lorentzian time, $\tau \to it$. For a detailed discussion of this aspect, we refer the reader to Appendixes A and B of [70].

The integral (A6) is divergent for $m=0$ and $\epsilon=0$. However, its derivatives are well defined and can be expressed analytically. After performing integration over k and q in turn, we obtain, in Euclidean signature,

$$\partial_\tau\langle\phi(\tau,x,y)\phi(0,0,0)\rangle = \frac{\sqrt{\mu\mu_0}}{A(2\pi)^2\tau}(\exp(u)Ei(-u)$$

$$+ \exp(-u)Ei(u)), \tag{A7}$$

where $u = xy\sqrt{\mu\mu_0}/\tau$, and $Ei(u)$ is the exponential integral. By analytical continuation, we obtain, in the Lorentzian signature,

$$\partial_t\langle\phi(t,x,y)\phi(0,0,0)\rangle = \frac{\sqrt{\mu\mu_0}}{2A\pi^2 t}(\cos(u)Ci(u) - \sin(u)Si(u)), \tag{A8}$$

where $u = xy\sqrt{\mu\mu_0}/t$ and $Si(u)$ and $Ci(u)$ are the trigonometric integrals.

APPENDIX B: FRACTONIC PROPAGATOR IN THE FINITE-VOLUME THEORY

Let us consider Euclidean theory (A1) on a $2+1$-dimensional torus $x \sim x + L_x$, $y \sim y + L_y$. Its Green's function is a solution to the following system with periodic boundary conditions

$$\begin{cases} A\left(-\mu_0\partial_\tau^2 - \epsilon(\partial_x^2 + \partial_y^2) - \frac{1}{\mu}\partial_x^2\partial_y^2 + \mu m^2\right)K(\vec{x}_1 - \vec{x}_2) = \delta^{(3)}(\vec{x}_1 - \vec{x}_2), \\ K(\tau, x+L_x, y) = K(\tau, x, y), \\ K(\tau, x, y+L_y) = K(\tau, x, y), \end{cases} \tag{B1}$$

where $\vec{x}_i = \{\tau_i, x_i, y_i\}$ are Euclidean 3-vectors. The solution can be written as an infinite series over the discrete spectrum of modes

$$\langle\phi(\tau,x,y)\phi(0,0,0)\rangle = \frac{1}{AL_xL_y}\sum_{n=-\infty}^{\infty}\sum_{s=-\infty}^{\infty}\int\frac{d\omega}{2\pi}\frac{e^{i\omega\tau+ik_nx+iq_sy}}{\mu_0\omega^2 + \epsilon(k_n^2+q_s^2) + \frac{1}{\mu}k_n^2q_s^2 + \mu m^2}, \tag{B2}$$

where $k_n = 2\pi n/L_x$ and $q_s = 2\pi s/L_y$ are Matsubara-like frequencies. It is only possible to evaluate analytically the integral over ω,

$$\int \frac{d\omega}{2\pi} \frac{e^{i\omega\tau}}{\omega^2 + \omega_{ns}^2} = \frac{1}{2|\omega_{ns}|} e^{-|\omega_{ns}|\cdot|\tau|} \equiv \frac{1}{2|\omega_{ns}|} e^{-|\omega_{ns}|\sqrt{\tau^2}}, \tag{B3}$$

which results in

$$\langle \phi(\tau,x,y)\phi(0,0,0)\rangle = \frac{1}{2AL_xL_y\mu_0} \sum_{n=-\infty}^{\infty} \sum_{s=-\infty}^{\infty} \sqrt{\frac{\mu_0\mu}{\epsilon\mu(k_n^2+q_s^2)+k_n^2q_s^2+\mu^2m^2}} e^{-\sqrt{\tau^2}\sqrt{\frac{\epsilon\mu(k_n^2+q_s^2)+k_n^2q_s^2+\mu^2m^2}{\mu_0\mu}}+ik_nx+iq_sy}, \tag{B4}$$

where we substitute $|\tau| \rightarrow \sqrt{\tau^2}$ as in (A6).

In fact, Eq. (B4) can be generalized onto the case of arbitrary free field dispersion relation $\omega_{ns} \equiv \omega(k_n, q_s)$,

$$\langle \phi(\tau,x,y)\phi(0,0,0)\rangle = \frac{1}{AL_xL_y} \sum_{n=-\infty}^{\infty} \sum_{s=-\infty}^{\infty} \frac{e^{-\omega_{ns}\sqrt{\tau^2}+ik_nx+iq_sy}}{2\omega_{ns}}. \tag{B5}$$

Taking into account that both relativistic, $\omega_{ns} = \sqrt{k_n^2 + q_s^2 + m^2}$, and regularized fractonic, $\omega_{ns} = \sqrt{\epsilon\mu(k_n^2+q_s^2)+k_n^2q_s^2+\mu^2m^2}/\sqrt{\mu_0\mu}$, discrete dispersion relations are symmetric under the sign inversion of n and s, we can transform this expression to

$$\langle \phi(\tau,x,y)\phi(0,0,0)\rangle = \frac{1}{AL_xL_y} \cdot \frac{e^{-\omega_0\sqrt{\tau^2}}}{2\omega_0} + \frac{1}{AL_xL_y} \sum_{n=1}^{\infty} (\cos(k_nx)+\cos(k_ny)) \cdot \frac{e^{-\omega_n\sqrt{\tau^2}}}{\omega_n}$$
$$+ \frac{2}{AL_xL_y} \sum_{n=1}^{\infty} \sum_{s=1}^{\infty} \cos(k_nx)\cos(q_sy) \cdot \frac{e^{-\omega_{ns}\sqrt{\tau^2}}}{\omega_{ns}}, \tag{B6}$$

where $\omega_0 = m$ and $\omega_n = \sqrt{k_n^2 + m^2}$ for the relativistic dispersion relation and $\omega_n = \sqrt{\epsilon\mu k_n^2 + \mu^2 m^2}/\sqrt{\mu\mu_0}$ for the regularized fractonic dispersion relation.

APPENDIX C: FRACTONIC ENERGY DENSITY AND DIPOLE MOMENT

In the mostly minus signature, the Lagrangian density of the relativistic massive scalar field theory is given by

$$\mathcal{L} = \frac{1}{2}g^{\mu\nu}\partial_\mu\phi\partial_\nu\phi - \frac{1}{2}m^2\phi^2 = \frac{1}{2}(\dot{\phi}^2 - (\nabla\phi)^2 - m^2\phi^2), \tag{C1}$$

leading to the energy density following from the Noether theorem

$$\mathcal{E} = \frac{\delta\mathcal{L}}{\delta(\partial^0\phi)}\partial_0\phi - g_{00}\mathcal{L} = \frac{1}{2}(\dot{\phi}^2 + (\nabla\phi)^2 + m^2\phi^2). \tag{C2}$$

In the mostly plus signature, the corresponding Lagrangian density and the energy density take the form

$$\mathcal{L} = -\frac{1}{2}g^{\mu\nu}\partial_\mu\phi\partial_\nu\phi - \frac{1}{2}m^2\phi^2 = \frac{1}{2}(\dot{\phi}^2 - (\nabla\phi)^2 - m^2\phi^2), \tag{C3}$$

and

$$\mathcal{E} = -\frac{\delta\mathcal{L}}{\delta(\partial^0\phi)}\partial_0\phi + g_{00}\mathcal{L} = \frac{1}{2}(\dot{\phi}^2 + (\nabla\phi)^2 + m^2\phi^2). \tag{C4}$$

In the Euclidean metric $(t \rightarrow -i\tau, \; g_{00} \rightarrow -g_{00}, \; \partial_0\phi \rightarrow i\partial_0\phi)$, we get

$$\mathcal{L} = \frac{1}{2}(\dot{\phi}^2 + (\nabla\phi)^2 + m^2\phi^2), \tag{C5}$$

and

$$\mathcal{E} = -\frac{\delta\mathcal{L}}{\delta(\partial^0\phi)}\partial_0\phi + g_{00}\mathcal{L} = \frac{1}{2}(-\dot{\phi}^2 + (\nabla\phi)^2 + m^2\phi^2). \tag{C6}$$

In the same way, we obtain the following expressions for the Euclidean fracton field theory:

$$\mathcal{L} = \frac{1}{2}\left(\mu_0(\partial_\tau\phi)^2 + \frac{1}{\mu}(\partial_x\partial_y\phi)^2 + \mu m^2\phi^2\right) \tag{C7}$$

and

$$\mathcal{E} = -\frac{\delta \mathcal{L}}{\delta(\partial^0 \phi)} \partial_0 \phi + g_{00} \mathcal{L}$$
$$= \frac{1}{2} \left(-\mu_0 \dot{\phi}^2 + \frac{1}{\mu} (\partial_x \partial_y \phi)^2 + \mu m^2 \phi^2 \right). \qquad \text{(C8)}$$

Then, the Euclidean energy density can be calculated by applying Wick's theorem to the two-point function,

$$\langle \mathcal{E} \rangle_\phi = -\frac{\langle \phi(\varepsilon, 0, 0) \partial_\tau \phi(\tau, x, y) \rangle \langle \partial_\tau \phi(\tau, x, y) \phi(-\varepsilon, 0, 0) \rangle}{\langle \phi(\varepsilon, 0, 0) \phi(-\varepsilon, 0, 0) \rangle}$$
$$+ \frac{\langle \phi(\varepsilon, 0, 0) \partial_x \phi(\tau, x, y) \rangle \langle \partial_x \phi(\tau, x, y) \phi(-\varepsilon, 0, 0) \rangle}{\langle \phi(\varepsilon, 0, 0) \phi(-\varepsilon, 0, 0) \rangle}$$
$$+ \frac{\langle \phi(\varepsilon, 0, 0) \partial_y \phi(\tau, x, y) \rangle \langle \partial_y \phi(\tau, x, y) \phi(-\varepsilon, 0, 0) \rangle}{\langle \phi(\varepsilon, 0, 0) \phi(-\varepsilon, 0, 0) \rangle}$$
$$+ \frac{m^2 \langle \phi(\varepsilon, 0, 0) \phi(\tau, x, y) \rangle \langle \phi(\tau, x, y) \phi(-\varepsilon, 0, 0) \rangle}{\langle \phi(\varepsilon, 0, 0) \phi(-\varepsilon, 0, 0) \rangle}.$$
$$\text{(C9)}$$

The remaining correlation functions are to be calculated from the momentum-space two-point function by Fourier transform,

$$\langle \partial_\tau \phi(\tau, x, y) \phi(\tau_0, 0, 0) \rangle$$
$$= -\frac{\tau - \tau_0}{2A\sqrt{(\tau - \tau_0)^2}} \int \frac{dkdq}{(2\pi)^2} e^{-\omega\sqrt{(\tau-\tau_0)^2}+ikx+iqy}, \qquad \text{(C10)}$$

$$\langle \partial_x \phi(\tau, x, y) \phi(\tau_0, 0, 0) \rangle = \frac{i}{A} \int \frac{dkdq}{(2\pi)^2} \frac{ke^{-\omega\sqrt{(\tau-\tau_0)^2}+ikx+iqy}}{2\omega}$$
$$\text{(C11)}$$

and

$$\langle \partial_x \partial_y \phi(\tau, x, y) \phi(\tau_0, 0, 0) \rangle$$
$$= -\frac{1}{A} \int \frac{dkdq}{(2\pi)^2} \frac{kqe^{-\omega\sqrt{(\tau-\tau_0)^2}+ikx+iqy}}{2\omega}. \qquad \text{(C12)}$$

We are also interested in the dipole momentum, which is globally conserved in pure fractonic theories. In the Lorentzian signature, the dipole current is given by [8]

$$J_0 = \mu_0 \partial_t \phi,$$
$$J^{xy} = -\frac{1}{\mu} \partial^x \partial^y \phi \qquad \text{(C13)}$$

with the conservation law

$$\partial_0 J = \partial_x \partial_y J^{xy}. \qquad \text{(C14)}$$

In this paper, we consider the square of the zero component of the current, J_0^2,

$$\langle J_0^2 \rangle = \frac{\langle \phi(i\varepsilon, 0, 0) | (\partial_t \phi_0(t, x, y))^2 | \phi(-i\varepsilon, 0, 0) \rangle}{\langle \phi(i\varepsilon, 0, 0) \phi(-i\varepsilon, 0, 0) \rangle}. \qquad \text{(C15)}$$

The correlation function has a form similar to that of ϕ^2 condensate (14) and thus can be calculated in the same way,

$$\langle J_0^2 \rangle = \frac{\left| \int dkdq e^{-\omega\sqrt{(\varepsilon-it)^2}+ikx+iqy} \right|^2}{4A\pi^2 \int dkdq\, \omega^{-1} e^{-2\varepsilon\omega}}. \qquad \text{(C16)}$$

In the case of finite volume, the integral over momenta is changed to the sum over Fourier modes.

[1] M. Pretko, Emergent gravity of fractons: Mach's principle revisited, Phys. Rev. D **96**, 024051 (2017).

[2] G. B. Halász, T. H. Hsieh, and L. Balents, Fracton topological phases from strongly coupled spin chains, Phys. Rev. Lett. **119**, 257202 (2017).

[3] A. Prem, M. Pretko, and R. Nandkishore, Emergent phases of fractonic matter, Phys. Rev. B **97**, 085116 (2018).

[4] R. M. Nandkishore and M. Hermele, Fractons, Annu. Rev. Condens. Matter Phys. **10**, 295 (2019).

[5] M. Pretko, X. Chen, and Y. You, Fracton phases of matter, Int. J. Mod. Phys. A **35**, 2030003 (2020).

[6] A. Gromov and L. Radzihovsky, Fracton matter, Rev. Mod. Phys. **96**, 011001 (2024).

[7] M. Pretko, The fracton gauge principle, Phys. Rev. B **98**, 115134 (2018).

[8] N. Seiberg and S.-H. Shao, Exotic symmetries, duality, and fractons in 2 + 1-dimensional quantum field theory, SciPost Phys. **10**, 027 (2021).

[9] N. Seiberg and S.-H. Shao, Exotic $U(1)$ symmetries, duality, and fractons in 3 + 1-dimensional quantum field theory, SciPost Phys. **9**, 046 (2020).

[10] J. Distler, M. Jafry, A. Karch, and A. Raz, Interacting fractons in 2 + 1-dimensional quantum field theory, J. High Energy Phys. 03 (2022) 070; 03 (2023) 115(E).

[11] P. Calabrese and J. L. Cardy, Time-dependence of correlation functions following a quantum quench, Phys. Rev. Lett. **96**, 136801 (2006).

[12] P. Calabrese and J. Cardy, Quantum quenches in extended systems, J. Stat. Mech. (2007) P06008.

[13] S. R. Das, D. A. Galante, and R. C. Myers, Universal scaling in fast quantum quenches in conformal field theories, Phys. Rev. Lett. **112,** 171601 (2014).

[14] S. R. Das, D. A. Galante, and R. C. Myers, Universality in fast quantum quenches, J. High Energy Phys. 02 (2015) 167.

[15] P. Calabrese and J. Cardy, Quantum quenches in $1+1$ dimensional conformal field theories, J. Stat. Mech. (2016) 064003.

[16] S. Sotiriadis, P. Calabrese, and J. Cardy, Quantum quench from a thermal initial state, Europhys. Lett. **87,** 20002 (2009).

[17] S. Sotiriadis and J. Cardy, Quantum quench in interacting field theory: A self-consistent approximation, Phys. Rev. B **81,** 134305 (2010).

[18] M. A. Rajabpour and S. Sotiriadis, Quantum quench in long-range field theories, Phys. Rev. B **91,** 045131 (2015).

[19] S. R. Das, D. A. Galante, and R. C. Myers, Smooth and fast versus instantaneous quenches in quantum field theory, J. High Energy Phys. 08 (2015) 073.

[20] S. R. Das, D. A. Galante, and R. C. Myers, Quantum quenches in free field theory: Universal scaling at any rate, J. High Energy Phys. 05 (2016) 164.

[21] M. R. Mohammadi Mozaffar and A. Mollabashi, Entanglement evolution in Lifshitz-type scalar theories, J. High Energy Phys. 01 (2019) 137.

[22] M. R. Mohammadi Mozaffar and A. Mollabashi, Universal scaling in fast quenches near Lifshitz-like fixed points, Phys. Lett. B **797,** 134906 (2019).

[23] M. R. M. Mozaffar and A. Mollabashi, Time scaling of entanglement in integrable scale-invariant theories, Phys. Rev. Res. **4,** L022010 (2022).

[24] M. M. Islam, K. Sengupta, and R. Sensarma, Non-equilibrium dynamics of bosons with dipole symmetry: A large N Keldysh approach, Phys. Rev. B **108,** 214314 (2023).

[25] D. S. Ageev and V. V. Pushkarev, Quantum quenches in fractonic field theories, arXiv:2306.14951.

[26] U. H. Danielsson, E. Keski-Vakkuri, and M. Kruczenski, Black hole formation in AdS and thermalization on the boundary, J. High Energy Phys. 02 (2000) 039.

[27] V. Balasubramanian, A. Bernamonti, J. de Boer, N. Copland, B. Craps, E. Keski-Vakkuri, B. Muller, A. Schafer, M. Shigemori, and W. Staessens, Thermalization of strongly coupled field theories, Phys. Rev. Lett. **106,** 191601 (2011).

[28] V. Balasubramanian, A. Bernamonti, J. de Boer, N. Copland, B. Craps, E. Keski-Vakkuri, B. Muller, A. Schafer, M. Shigemori, and W. Staessens, Holographic thermalization, Phys. Rev. D **84,** 026010 (2011).

[29] D. S. Ageev and I. Y. Aref'eva, Holographic non-equilibrium heating, J. High Energy Phys. 03 (2018) 103.

[30] D. S. Ageev and I. Y. Aref'eva, Waking and scrambling in holographic heating up, Teor. Mat. Fiz. **193,** 146 (2017).

[31] P. Calabrese and J. Cardy, Entanglement and correlation functions following a local quench: A conformal field theory approach, J. Stat. Mech. (2007) P10004.

[32] J.-M. Stéphan and J. Dubail, Local quantum quenches in critical one-dimensional systems: Entanglement, the Loschmidt echo, and light-cone effects, J. Stat. Mech. (2011) P08019.

[33] M. Ganahl, E. Rabel, F. H. L. Essler, and H. G. Evertz, Observation of complex bound states in the spin-1/2 Heisenberg *XXZ* chain using local quantum quenches, Phys. Rev. Lett. **108,** 077206 (2012).

[34] A. Bayat, B. Alkurtass, P. Sodano, H. Johannesson, and S. Bose, Measurement quench in many-body systems, Phys. Rev. Lett. **121,** 030601 (2018).

[35] M. Gruber and V. Eisler, Magnetization and entanglement after a geometric quench in the XXZ chain, Phys. Rev. B **99,** 174403 (2019).

[36] L. Rossi, F. Dolcini, F. Cavaliere, N. Traverso Ziani, M. Sassetti, and F. Rossi, Signature of generalized Gibbs ensemble deviation from equilibrium: Negative absorption induced by a local quench, Entropy **23,** 220 (2021).

[37] P. Calabrese and J. L. Cardy, Evolution of entanglement entropy in one-dimensional systems, J. Stat. Mech. (2005) P04010.

[38] P. Caputa, J. Simón, A. Štikonas, and T. Takayanagi, Quantum entanglement of localized excited states at finite temperature, J. High Energy Phys. 01 (2015) 102.

[39] S. He, T. Numasawa, T. Takayanagi, and K. Watanabe, Quantum dimension as entanglement entropy in two dimensional conformal field theories, Phys. Rev. D **90,** 041701 (2014).

[40] M. Nozaki, T. Numasawa, and T. Takayanagi, Quantum entanglement of local operators in conformal field theories, Phys. Rev. Lett. **112,** 111602 (2014).

[41] J. S. Cotler, M. P. Hertzberg, M. Mezei, and M. T. Mueller, Entanglement growth after a global quench in free scalar field theory, J. High Energy Phys. 11 (2016) 166.

[42] D. S. Ageev and I. Y. Aref'eva, When things stop falling, chaos is suppressed, J. High Energy Phys. 01 (2019) 100.

[43] B. Doyon, A. Lucas, K. Schalm, and M. J. Bhaseen, Non-equilibrium steady states in the Klein-Gordon theory, J. Phys. A **48,** 095002 (2015).

[44] A. F. Astaneh and A. E. Mosaffa, Quantum local quench, AdS/BCFT and Yo-Yo string, J. High Energy Phys. 05 (2015) 107.

[45] P. Caputa, M. Nozaki, and T. Takayanagi, Entanglement of local operators in large-N conformal field theories, Prog. Theor. Exp. Phys. **2014,** 093B06 (2014).

[46] C. T. Asplund, A. Bernamonti, F. Galli, and T. Hartman, Holographic entanglement entropy from 2d CFT: Heavy states and local quenches, J. High Energy Phys. 02 (2015) 171.

[47] W.-Z. Guo and S. He, Rényi entropy of locally excited states with thermal and boundary effect in 2D CFTs, J. High Energy Phys. 04 (2015) 099.

[48] P. Caputa, J. Simón, A. Štikonas, T. Takayanagi, and K. Watanabe, Scrambling time from local perturbations of the eternal BTZ black hole, J. High Energy Phys. 08 (2015) 011.

[49] P. Caputa and A. Veliz-Osorio, Entanglement constant for conformal families, Phys. Rev. D **92,** 065010 (2015).

[50] B. Chen, W.-Z. Guo, S. He, and J.-q. Wu, Entanglement entropy for descendent local operators in 2D CFTs, J. High Energy Phys. 10 (2015) 173.

[51] D. S. Ageev, I. Y. Aref'eva, and M. D. Tikhanovskaya, $(1 + 1)$-correlators and moving massive defects, Theor. Math. Phys. **188,** 1038 (2016).

[52] D. S. Ageev and I. Y. Aref'eva, Holographic instant conformal symmetry breaking by colliding conical defects, Theor. Math. Phys. **189,** 1742 (2016).

[53] M. Rangamani, M. Rozali, and A. Vincart-Emard, Dynamics of holographic entanglement entropy following a local quench, J. High Energy Phys. 04 (2016) 069.

[54] P. Caputa, M. Nozaki, and T. Numasawa, Charged entanglement entropy of local operators, Phys. Rev. D **93,** 105032 (2016).

[55] F. Franchini, A. Gromov, M. Kulkarni, and A. Trombettoni, Universal dynamics of a soliton after an interaction quench, J. Phys. A **48,** 28FT01 (2015).

[56] F. Franchini, M. Kulkarni, and A. Trombettoni, Hydrodynamics of local excitations after an interaction quench in 1D cold atomic gases, New J. Phys. **18,** 115003 (2016).

[57] S. He, Conformal bootstrap to Rényi entropy in 2D Liouville and super-Liouville CFTs, Phys. Rev. D **99,** 026005 (2019).

[58] W.-Z. Guo, S. He, and Z.-X. Luo, Entanglement entropy in $(1 + 1)$D CFTs with multiple local excitations, J. High Energy Phys. 05 (2018) 154.

[59] D. S. Ageev, I. Y. Aref'eva, A. A. Bagrov, and M. I. Katsnelson, Holographic local quench and effective complexity, J. High Energy Phys. 08 (2018) 071.

[60] T. Shimaji, T. Takayanagi, and Z. Wei, Holographic quantum circuits from splitting/joining local quenches, J. High Energy Phys. 03 (2019) 165.

[61] L. Apolo, S. He, W. Song, J. Xu, and J. Zheng, Entanglement and chaos in warped conformal field theories, J. High Energy Phys. 04 (2019) 009.

[62] D. S. Ageev, Holography, quantum complexity and quantum chaos in different models, EPJ Web Conf. **191,** 06006 (2018).

[63] P. Caputa, T. Numasawa, T. Shimaji, T. Takayanagi, and Z. Wei, Double local quenches in 2D CFTs and gravitational force, J. High Energy Phys. 09 (2019) 018.

[64] S. He and H. Shu, Correlation functions, entanglement and chaos in the $T\bar{T}/J\bar{T}$-deformed CFTs, J. High Energy Phys. 02 (2020) 088.

[65] A. Bhattacharyya, T. Takayanagi, and K. Umemoto, Universal local operator quenches and entanglement entropy, J. High Energy Phys. 11 (2019) 107.

[66] S. He, Note on higher-point correlation functions of the $T\bar{T}$ or $J\bar{T}$ deformed CFTs, Sci. China Phys. Mech. Astron. **64,** 291011 (2021).

[67] N. Zenoni, R. Auzzi, S. Caggioli, M. Martinelli, and G. Nardelli, A falling magnetic monopole as a holographic local quench, J. High Energy Phys. 11 (2021) 048.

[68] K. Suzuki and T. Takayanagi, BCFT and islands in two dimensions, J. High Energy Phys. 06 (2022) 095.

[69] M. Nozaki, T. Numasawa, and T. Takayanagi, Holographic local quenches and entanglement density, J. High Energy Phys. 05 (2013) 080.

[70] D. S. Ageev, A. I. Belokon, and V. V. Pushkarev, From locality to irregularity: Introducing local quenches in massive scalar field theory, J. High Energy Phys. 05 (2023) 188.

[71] A. Paramekanti, L. Balents, and M. P. A. Fisher, Ring exchange, the exciton Bose liquid, and bosonization in two dimensions, Phys. Rev. B **66,** 054526 (2002).

[72] M. Cramer, A. Serafini, and J. Eisert, Locality of dynamics in general harmonic quantum systems, arXiv:0803.0890.

[73] M. V. Berry and S. Klein, Integer, fractional and fractal Talbot effects, J. Mod. Opt. **43,** 2139 (1996).

[74] B. Dubuc, J. F. Quiniou, C. Roques-Carmes, C. Tricot, and S. W. Zucker, Evaluating the fractal dimension of profiles, Phys. Rev. A **39,** 1500 (1989).

[75] D. S. Ageev, A. A. Bagrov, and A. A. Iliasov, Deterministic chaos and fractal entropy scaling in Floquet conformal field theories, Phys. Rev. B **103,** L100302 (2021).

[76] D. S. Ageev and V. V. Pushkarev (to be published).